IDENTIFICATION AND DEVELOPMENT OF TUNAS, BILLFISHES AND ROUGHIES

Fishing Industry Research and Development Council : Project Final Report 1993

PROJECT SUPERVISOR
Associate Professor A. Clive Crossley, B.Sc. Ph.D.(Cantab).
School of Biological Sciences
Zoology Building A08,
University of Sydney,
N.S.W. 2006.

ABSTRACT

Eighteen species of tuna and billfish larvae collected in the Indian and Pacific Oceans, and material provided and identified by Dr Nishikawa of the Japanese Far Seas Fisheries Research Laboratory from "Shoyo Maru" cruises in the North Pacific Ocean, have been examined in the scanning electron microscope, with the intention of producing an atlas in which microstructure and melanophore patterns are related.. Sample micrographs from this atlas are presented.

Larvae and juveniles of four species of roughies (Trachichthyidae) from southern Australian waters have been examined using scanning electron microscopy. Differences in scale morphology allow these species to be identified. Electron micrographs of embryos and early larvae of orange roughy are also presented.

The density (specific gravity) of orange roughy eggs and embryos has been determined by neutral bouyancy in a calibrated density gradient column containing Ficoll and seawater. The specific gravity of seawater at depths up to 1200M was mimiced by the density gradient column, and the neutral bouyancy reading used to predict the vertical distribution of eggs and embryos in the ocean.

Eggs fertilized *in vitro* in surface 34.5 $^{o}/_{oo}$ seawater have an initial density of 1.0310 g/cm3 , equivalent to neutral bouyancy at about 400M. As these eggs develop, they become more dense, reaching a density of 1.0321 g/cm3 34 hours after fertilization. In terms of neutral bouyancy, this is equivalent to a depth of about 500M.

The specific gravity of the eggs is of primary importance in bouyancy, and the methodology developed in this project enables us to measure the specific gravity of individual eggs, and to use this information to predict the vertical distribution of eggs and embryos. In general neutral bouyancy measurements on living eggs using Ficoll-seawater density gradients corresponded approximately with the observed capture depth by EZ net sampling. It is likely that the Ficoll methodology will replace the conventional use of saline gradients, because of the reduced osmotic stress applied to the egg, particularly in columns mimicing a deep water column.

The structure of developing, unfertilized and fertilized eggs has been studied using the scanning electron microscope in order to establish what changes occur on maturation and fertilization. The ultrastructure of the egg chorion changes on fertilization. The microstructure of the orange roughy egg micropyle is related to the ultrastructure of the sperm. The dimensions and pitch aspect of the orange roughy sperm tail helix relate to the helix of the micropyle vestibule.

Vertebrate eye lens cells contain a number of proteins, collectively called crystallins, that change character during development and ageing. Protein synthesis takes place only in the outer cortex of the lens. As lens cells mature they become part of the lens nucleus and lose the ability to synthesize new crystallins. As a result , the central fibres of the lens contain proteins that are as old as the individual to which the eye belongs, whilst the more superficial fibres contain newly synthesized protein. This feature of lenses has made them ideal for distinguishing age-related changes in proteins occurring during synthesis from those occurring due to post-translational modification. Crystallin-like proteins in the orange roughy lens have been identified using HPLC and immunoblotting, and age-related changes have been identified. The results of the study are of general theoretical interest in an understanding of crystallins and ageing. Changes in lens crystallins may provide a novel methodology for determination of orange roughy lifespan. Changes in crystallins are related to changes in lens size and to growth of the otolith, which are documented here for the same individual fishes. Changes in the ultrastructure of orange roughy lenses and otoliths are also documented in relation to fish growth.

Fishing Industry Research and Development Council : Project Final Report 1993

PROJECT TITLE
Identification and Development of Tunas, Billfishes, and Roughies

PROJECT SUPERVISOR
Associate Professor A. Clive Crossley, B.Sc. Ph.D.(Cantab).
School of Biological Sciences,
Zoology Building AO8,
University of Sydney,
N.S.W. 2006.

ADMINISTRATIVE CONTACT
Name Ms Margaret Sager, Senior Administrative Officer,
Address Research Office, Mackie Building,
University of Sydney, Sydney, N.S.W. 2006.
Telephone (02)6924746. Fax. (02) 6923256

PROJECT OBJECTIVES

Objectives

A programme of microscopy and molecular analysis applied to Tuna, Billfish and Roughy embryos, larvae, juveniles and adults, designed to improve methods of identification and consequently management of species important in Australian fisheries.

Objective 1. To produce an improved system for identification of Tuna and Billfish, larvae, juveniles and adults, using a combination of electron microscopy and protein molecular biology.To develop an atlas of tuna larvae in which microstructure, melanophore patterns, and protein distribution patterns are related.

Objective 2. To identify the levels and locations in the bathypelagic region where embryonic and larval development of the Orange Roughy takes place, by means of bouyancy determinations on living embryos maintained at the surface. To capture and attempt to maintain embryos and larvae under conditions prevailing in the bathypelagic region. To provide light and electron micrographs and colour video images of orange roughy egg development stages and larvae, useful in the egg survey method.

FINAL REPORT CONTENTS

FINAL REPORT

1 Introduction

1.1 Project Timing

The project commenced on 6th February 1989 when I was advised that FIRDC funding for the project had been approved from 1st January 1989. This report covers the work carried out until the financial end of the project, on 31st December 1992. Data from the project is still being analysed and publications are expected to follow.

1.2 Report Aspects

There are two parallel aspects of the project which involve similar techniques. One aspect concerns tuna and billfish, and was the main thrust of the project in 1989-90, and has already been the subject of progress reports. A synopsis of this work is included here. The second aspect of the project concerned orange roughy development and ageing, and was the main thrust of the work in 1991-2. A more detailed report on this work is included for the first time here. Publications are in preparation in both areas of the project.

2 . Tuna and Billfish Identification

2.1 Introduction

The present system of identification of tuna and billfish larvae, based largely on melanophore patterns, is not definitive, and in particular presents serious difficulties when applied to two tunas important in the Australian fishery, the big-eye Tuna *T.obesus* and the southern bluefin tuna *T.maccoyii*. These difficulties are recognized in the 1987 CSIRO Report (#186) by Nishikawa and Rimmer, and lead in turn to difficulties in interpretation of the population data on tuna larvae on which management strategies may depend. What is needed is an atlas of scombroid larval anatomy, containing data on pigment distribution related to other microanatomical features such as dentition, otolith and caudal fin structure, and to a protein or other molecular "fingerprints".

2.2 Electron microscopy

During 1989 I completed examination of the larvae of nine scombroid species in the scanning electron microscope, using material collected by myself on a "Soela" Indian Ocean cruise in

1987, and material provided by Dr Nishikawa of the Japanese Far Seas Fisheries Research Laboratory from "Shoyo Maru" cruises in the North Pacific Ocean. In 1990 I joined a South Pacific Commission research ship "Te Tuatai" for 10 days with the purpose of collecting scombroid larvae from the south central Pacific for electron microscopy and comparison with Indian Ocean and N. Pacific specimens. Larval collections were made using a ring net deployed when the vessel was not engaged in tagging operations, and the collecting was very successful. (My report to the South Pacific Commission on this work forms Appendix 1 of this report). The collection of *T. obesus* larvae from an area without *T. maccoyii* was particularly useful, but many other species, including some as yet unidentified, were collected.

Techniques have been developed for preservation of tuna larvae in the 5-15mm length range, from samples collected at sea, for subsequent scanning electron microscopy. Electron micrographs reveal details of microanatomy that are not obvious in light micrographs, although magnification is not great, (**Figure 2.1**) and details, once established, are often visible in fresh material examined under a dissecting microscope . Comparison of living material, material preserved in glutaraldehyde for electron microscopy, and samples bulk fixed in alcohol or formalin, reveal the extent of post-mortem handling artefacts, and in fact allow us to get more information from bulk samples.

A micro-anatomical comparator for larvae of these species is in preparation , and will include drawings and electron micrographs as well as notes on dentition and pigmentation. This work is being prepared for publication, and will be forwarded as soon as it is available. **Figures 2.1- 2.6** refer to this work.

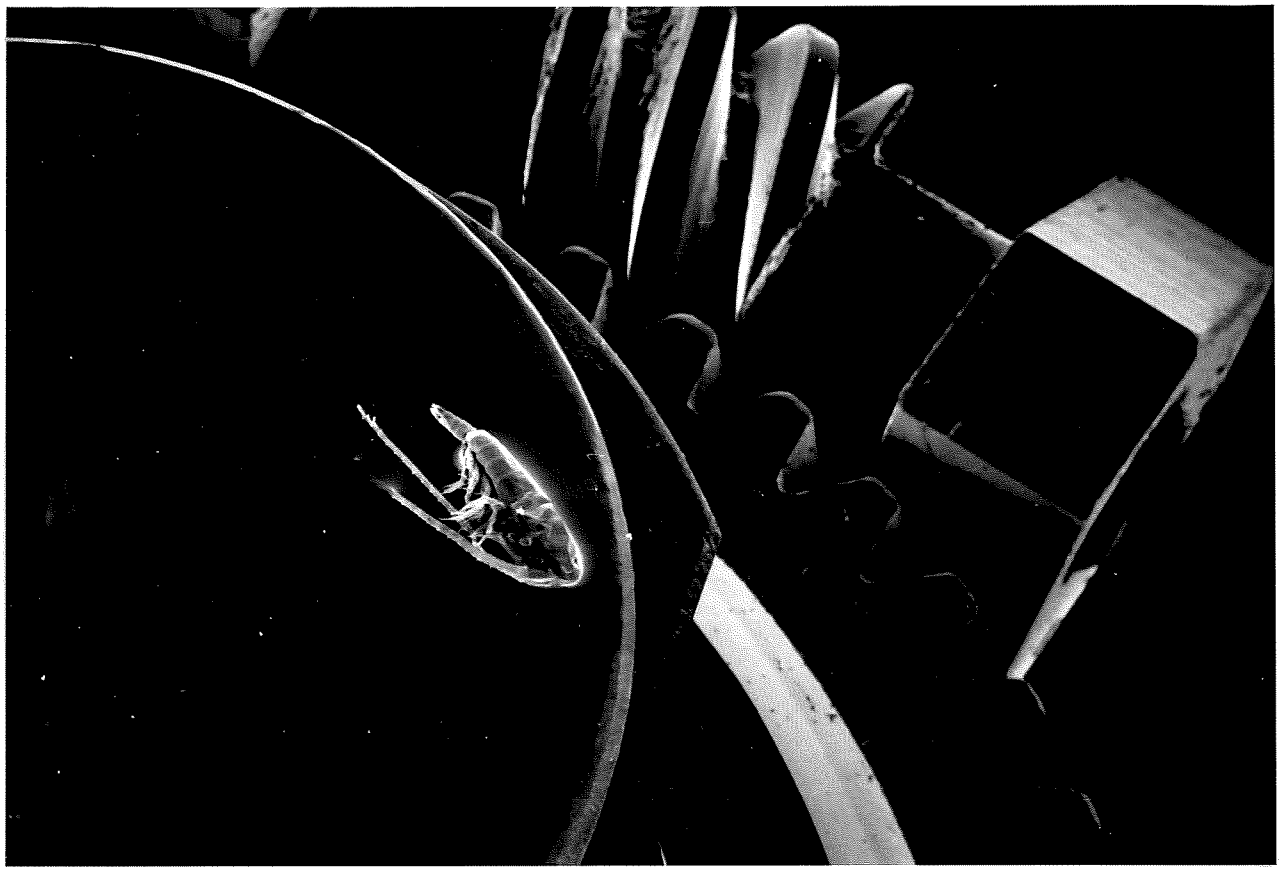

Figure 2.1 The scanning electron microscope is a useful tool for the demonstration of microstructure of fish larvae and small invertebrates. The depth of field available is shown in this micrograph of a crustacean 3mm in length resting on the rotating stage of the microscope.

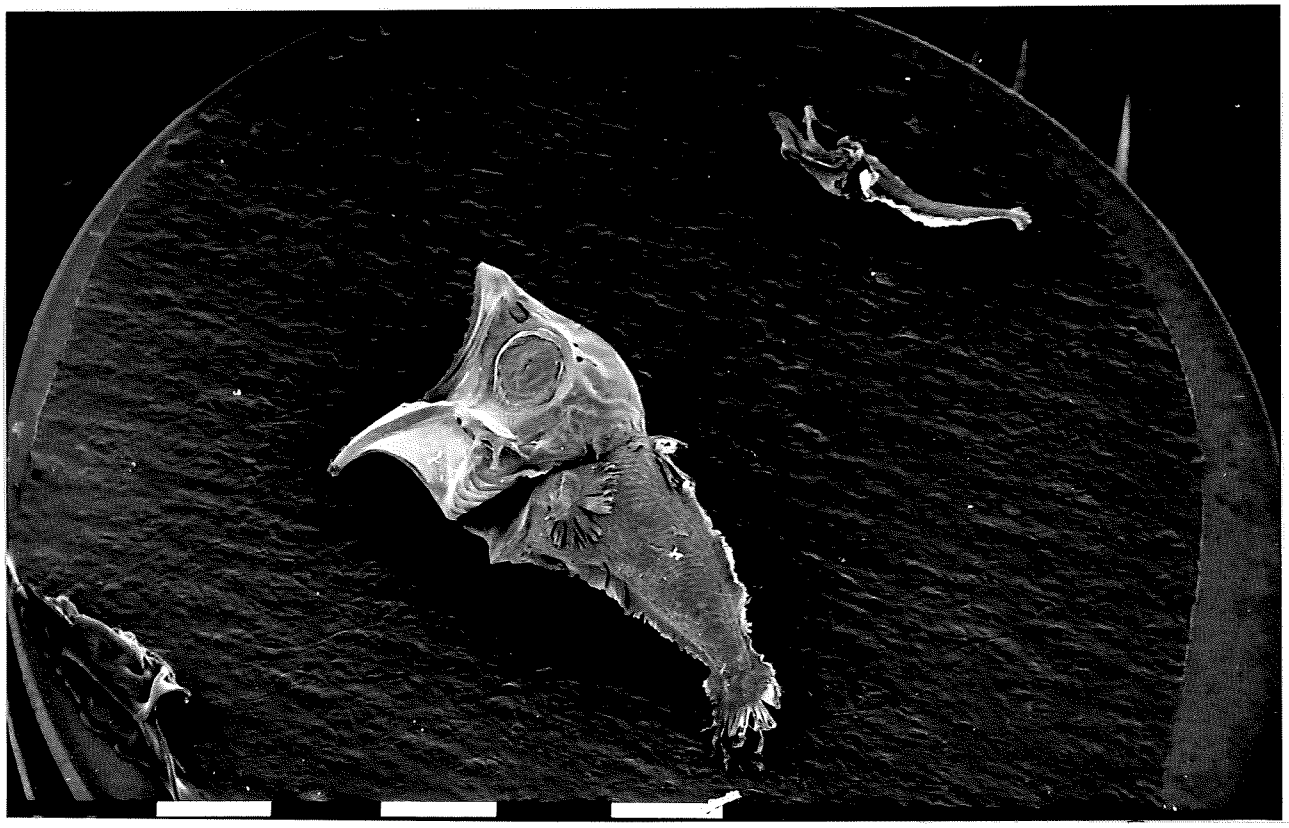

Figure 2.2 Tuna larvae on the rotating stage of the scanning electron microscope. Both are larvae of the Southern bluefin tuna *Thunnus maccoyii* . A 6 mm and a 4 mm larva are on the stage.

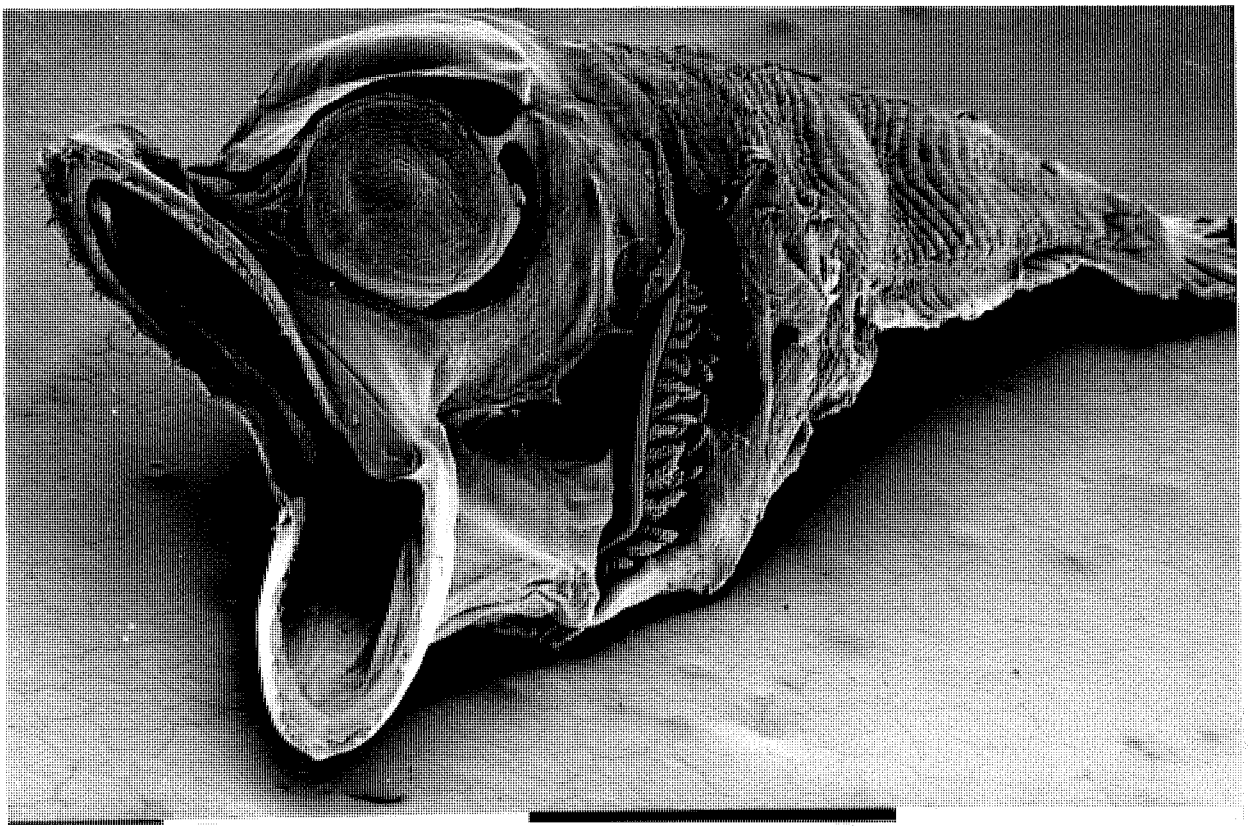

Figure 2.3 SEM of Southern blufin tuna *Thunnus maccoyii* 6 mm larva, captured in the north Indian Ocean. The open mouth allows detailed examination of the dentition.Gill structure and details of the myotome configuration are also visible. Scale bar represents 1mm.

Figure 2.4 Light micrograph of Southern blufin tuna *Thunnus maccoyii* 6 mm larva, captured in the north Indian Ocean. Some details of the melanophore pattern are visible. c.f. Figure 2.2

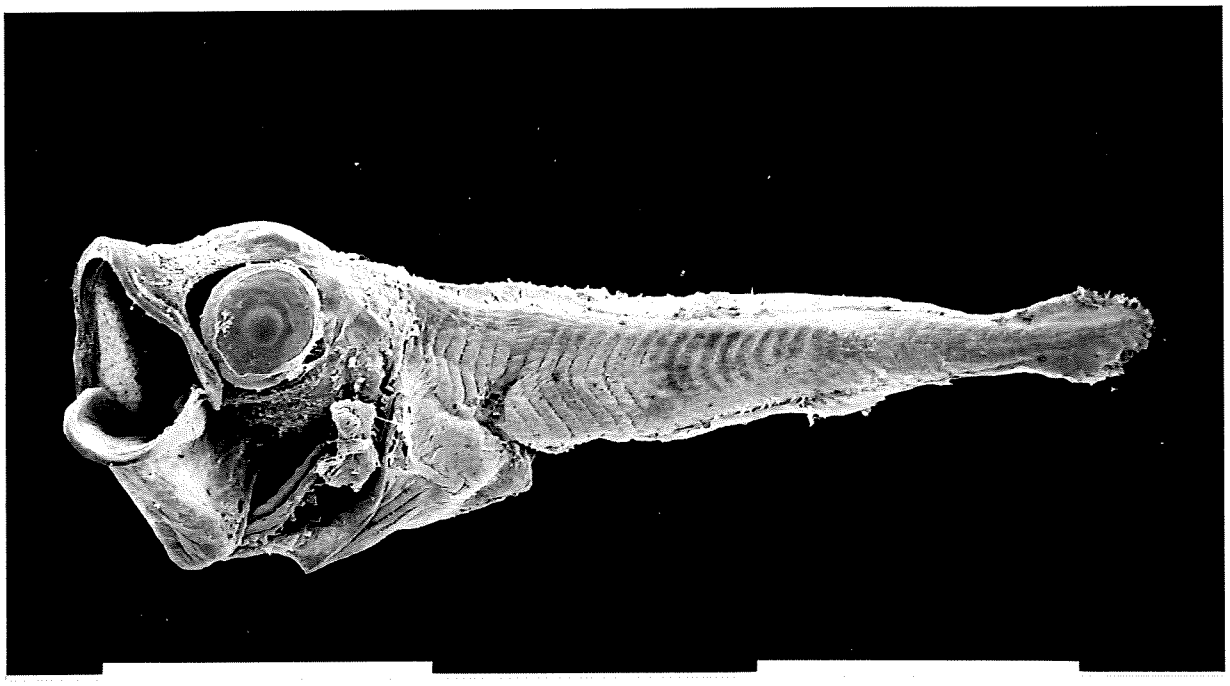

Figure 2.5 SEM of Yellowfin tuna *Thunnus albacares* 4 mm larva, captured in the central Pacific Ocean. Scale bar represents 1mm.

Figure 2.6 SEM of 6.5 mm larva of the Wahoo *Acanthocybium* from Java Sea. Note the long jaws and extended series of myotomes. Scale bar represents 1mm.

3 Identification of Roughy Larvae (1990-1)

At least four species of roughies (Trachichthydae) occur in Southern Australian Waters :*Trachichthys australis* the common roughy; *Optivus elongatus* the slender roughy; *Paratrachichthys trailli* the sandpaper fish, and *Hoplostethus atlanticus* the orange roughy. I have obtained specimens of larvae and juveniles of the first three species (identified by Dr Alan Jordan) for scanning electron microscopy and prepared electron micrographs of these species. Significant differences in scale morphology allow these species to be identified from the scales alone, once these develop, and other microanatomical features that are useful in larval identification stand out in micrographs.

Until 1990, no orange roughy larvae had been identified. Ring net samples in orange roughy aggregations in waters from 200M to 800M deep off St Helens Point, Tasmania, provided many eggs, but no larvae that were attributable to *Hoplostethus* had been captured. My work, and that of Dr. Alan Jordan on the other closely related roughy species make potential identification reasonably secure.

In July 1990 advanced embryos and very early larvae of Orange roughy were collected for the first time in ring net and bongo net tows carried out from "Tasmanian Enterprise" and "Megisti Star". However, as explained in the following section, no advanced larval or juvenile *Hoplostethus* were collected in 1990. **Figures 3.1-3.4** refer to this work.

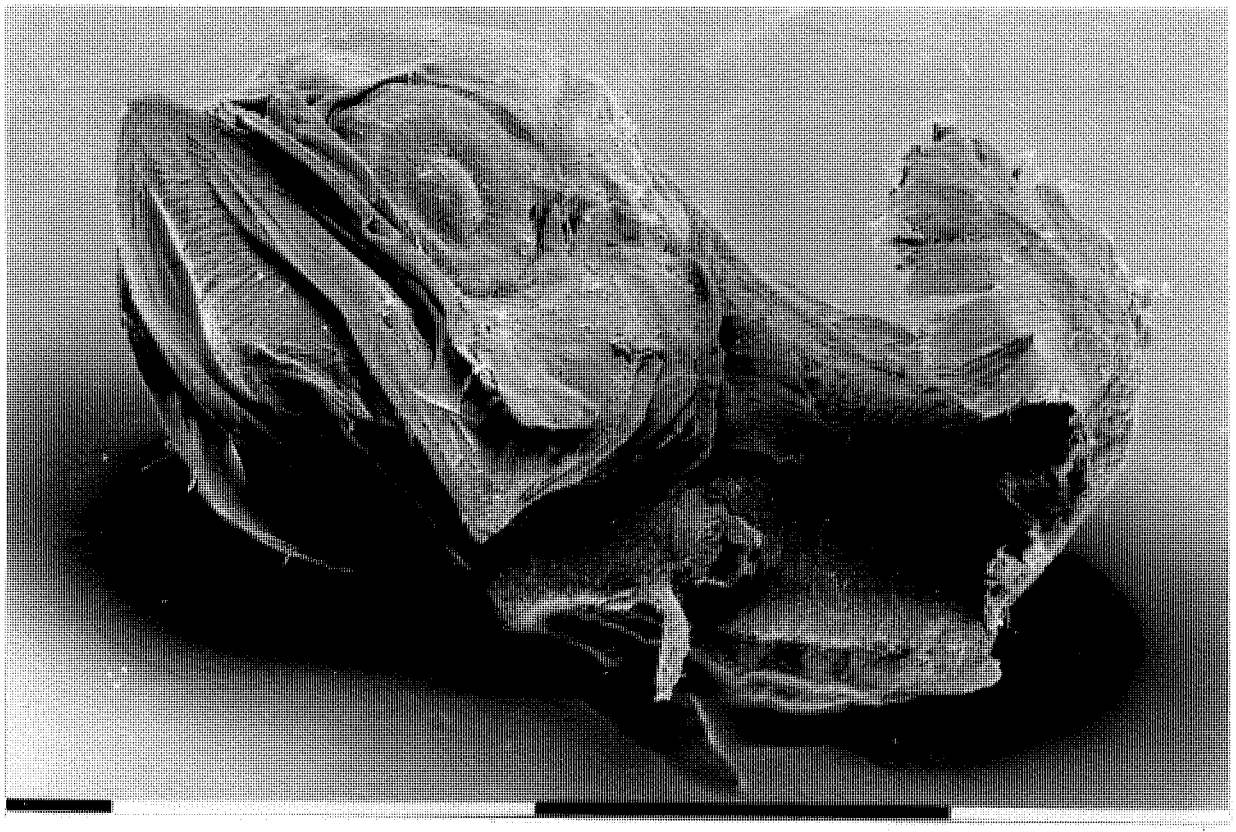

Figure 3.1 SEM of Slender Roughy *Optivus sp* (Pisces Trachichthyidae) larva length 4.3mm, ventral view . Scale bar represents 1 mm.

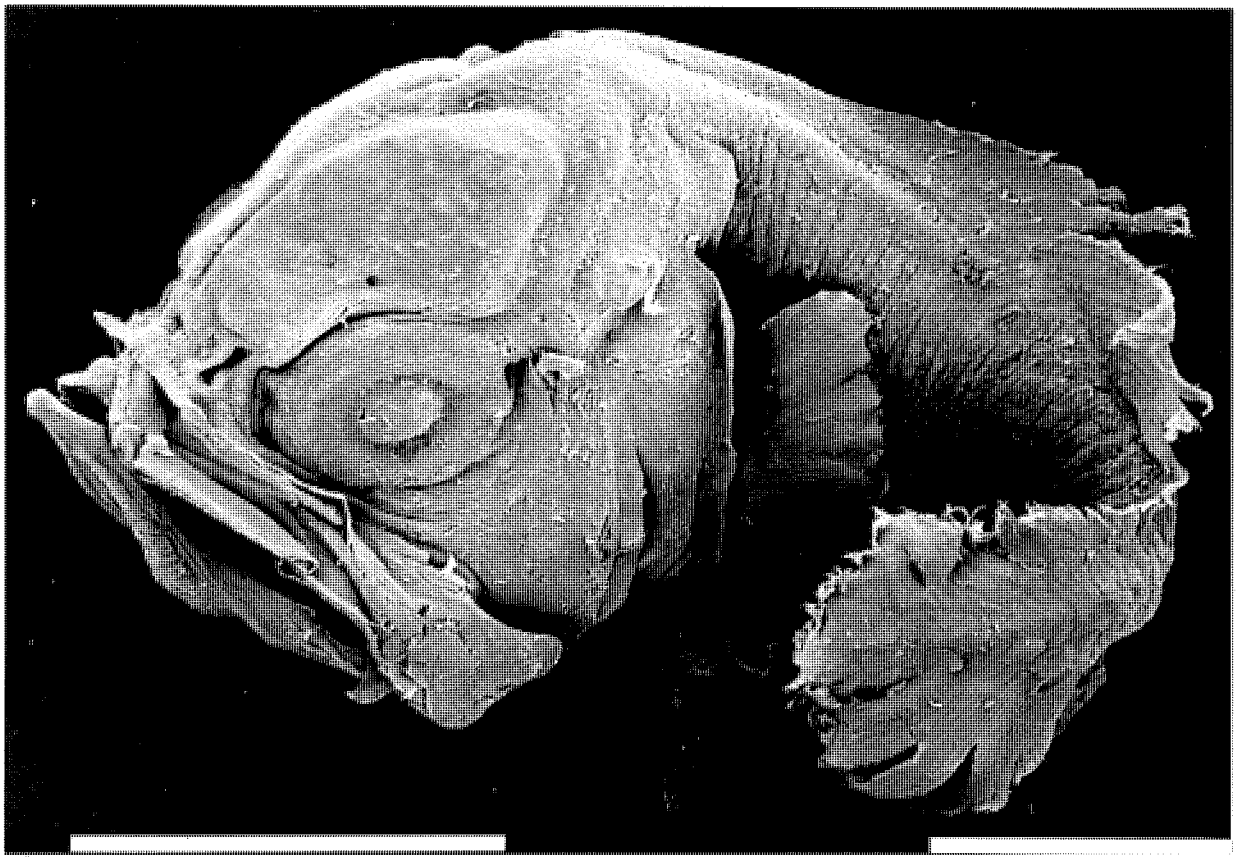

Figure 3.2 SEM of Slender Roughy *Optivus sp* (Pisces Trachichthyidae) larva length 4.3mm, dorsal view . Scale bar represents 1 mm.

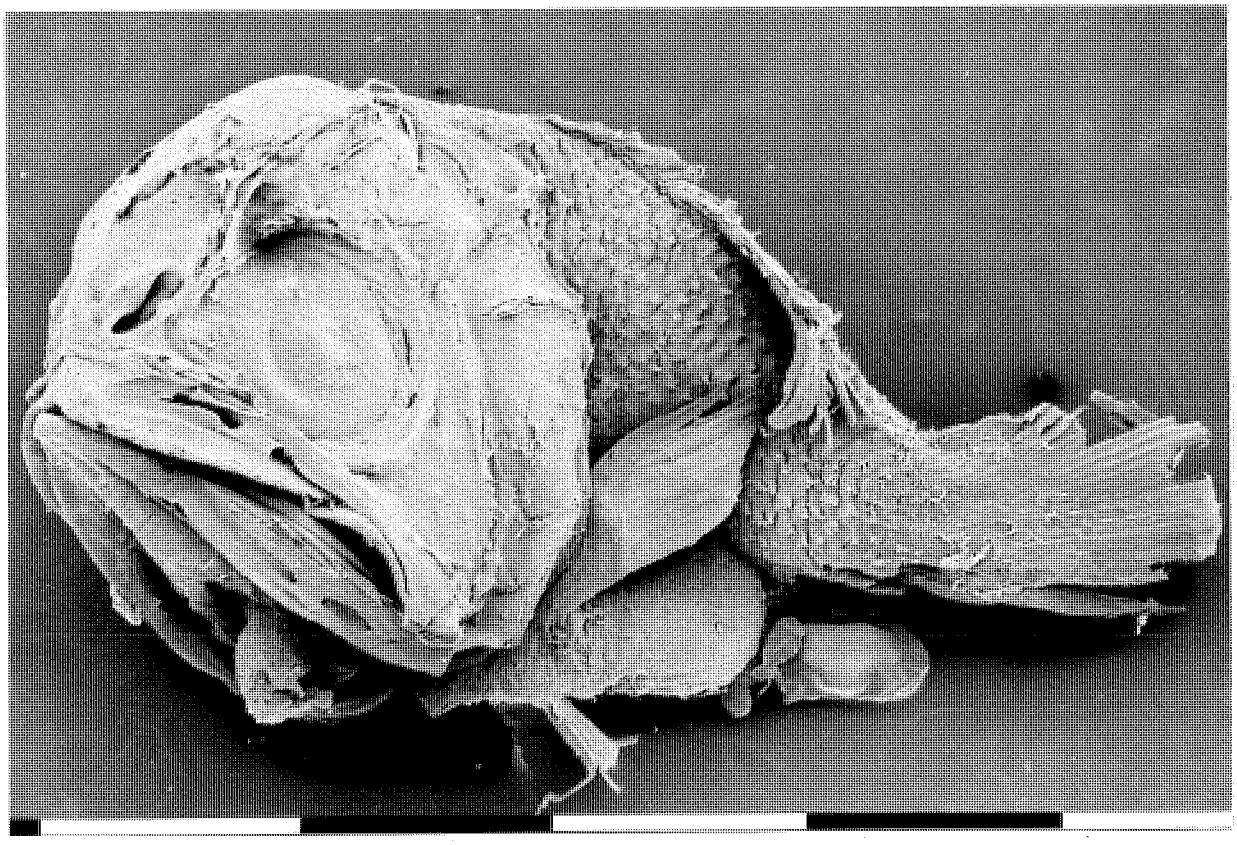

Figure 3.4 SEM of the Tasmanian Common Roughy *Paratrachichthys sp* (Pisces Trachichthyidae) juvenile length 60mm. View of jaws, teeth and snout . Scale bar represents 1 mm.

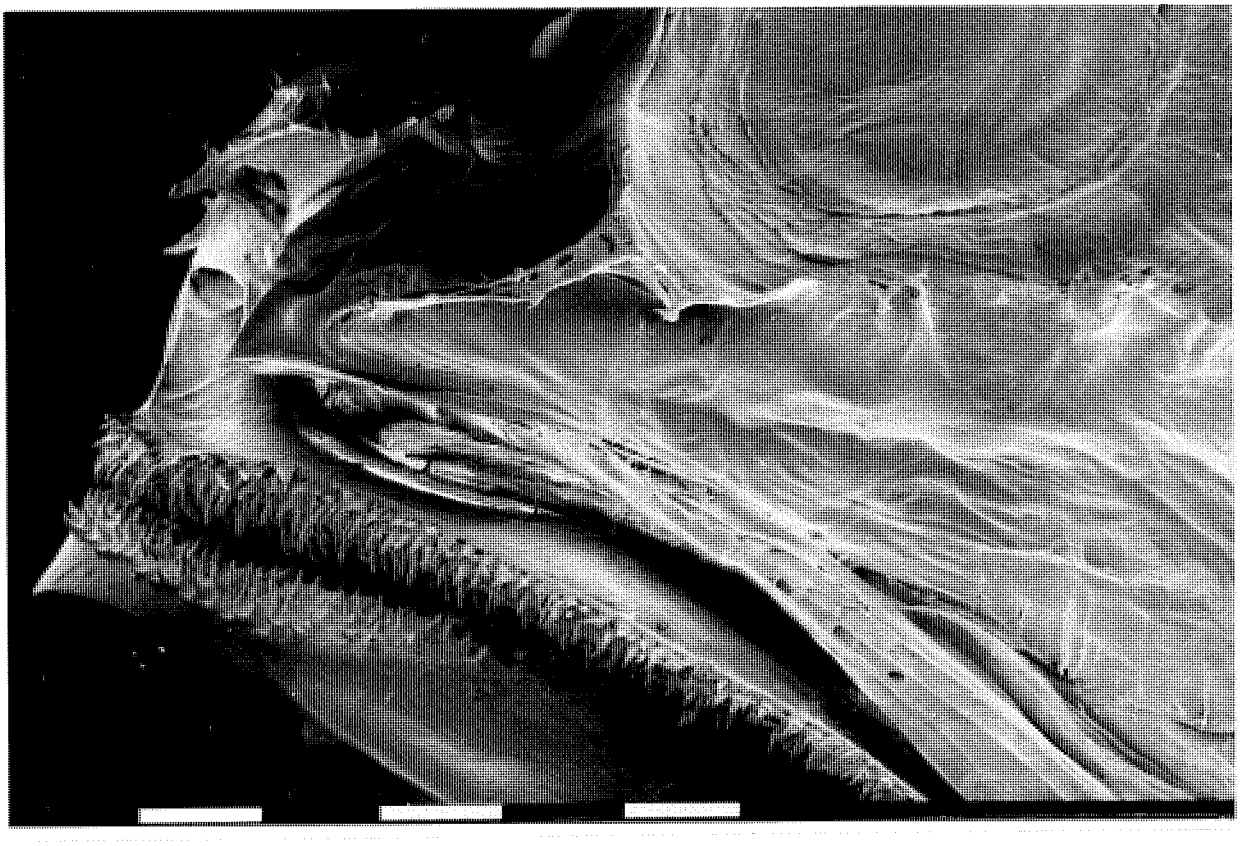

Figure 3.3 SEM of Slender Roughy *Optivus sp* (Pisces Trachichthyidae) larva length 5.4 mm, lateral view showing early development of scales . Scale bar represents 1 mm.

4 Development of Orange Roughy Eggs - Egg Survey Method.

4.1 Introduction

In 1989 I obtained orange roughy eggs by ring net sampling at 600M and by stripping captured mature females. These eggs were fertilized *in vitro* and used for preliminary developmental studies. These studies were undertaken in an attempt to rear orange roughy larvae. Although development to hatching was not obtained, two useful provisional observations were made. Firstly it was apparent that a small proportion of both captured and *in vitro* orange roughy eggs developed significantly (to gastrulation) when conserved in sea water at 6°C in the dark and at surface atmospheric pressure. Secondly, my observations indicated that fertilized orange roughy eggs sink in surface sea water at surface pressure. Both of these observations formed the basis for work in the 1990 spawning season, and were also relevant to the proposed development of an Egg Survey Method by CSIRO (Tony Koslow). Establishment of an accurate time scale for early embryonic development is critical for the validation of this method, and my observations indicate that although development continues under the given conditions at surface pressures, it is extremely slow, at least under the culture conditions employed. The implications of this are obviously that embryos may be carried well away from spawning aggregations before macroscopic changes are obvious. These preliminary results were important in the formulation of an experimental design for the 1990-2 spawning seasons.

4.2 Orange Roughy Egg and Embryo Density Determinations 1990-1 : The Problem

Orange Roughy adults in reproductive condition are trawled in large numbers from slope waters in the area of St Helens, Tasmania, with particular concentrations adjacent to a seamount (41 ° 13' S, 148 ° 45' E) at 600-800M depth. Open ring-net samples taken between 600M and the surface reveal numerous eggs, but few of the eggs taken appear to show developmental stages, such as cleavage or gastrulation and no larvae have been identified in surface waters. The questions that arise are :-

1. Where do orange roughy embryos and larvae develop ?
2. How localized is the developmental process in the spawning area ?
3. Do the embryos and larvae rise or sink in the water column ?

The answers to these questions are important for stock assessment, not only because we know very little about the reproductive cycle and recruitment in this species, but also because one of the proposed methods of adult stock assessment is the "Egg Survey Method", which depends *a priori* on accurate timing and staging of the embryonic development process.

4.3 Theory

The position of an egg or embryo in the water column depends primarily on its density. The density of seawater increases with depth, and this increase is dependent on salinity, temperature, and hydrostatic pressure. These parameters are known or can be estimated or measured for the watercolumn near St Helens seamount . The density of seawater can be altered without increasing the hydrostatic pressure by the addition of solutes. Most solutes such as salts, increase the osmotic pressure of the seawater and make it too hypertonic to allow survival of developing embryos. The key element in the present research strategy is to use the sucrose polymer Ficoll as the added solute, which increases the density of a solution without greatly increasing the osmolarity. There is a nearly linear relationship between the concentration of Ficoll and the density of a Ficoll solution. Increases in osmolarity due to Ficoll can be compensated by small reductions in salts in the seawater.

4.4 Application

In 1990 A.C. Crossley joined the chartered CSIRO research vessel "Megisti Star" and carried out a series of experiments between 26/07/90 - 30/07/90 . Ripe male and female fish in good condition were selected from trawl samples. Eggs were obtained from running ripe females and maintained in in the dark in seawater at 6^{o} C, the temperature of the ocean in which the fish had been living. Sperm from spawning males was maintained in seawater separately under identical conditions. After varying periods allowed for capacitation, samples were mixed for attempted *in vitro* fertilization. Ring net samples of naturally spawned and fertilized eggs were also maintained under identical conditions.

Unfertilized eggs, naturally spawned eggs and presumptive *in vitro* embryos were all used in density determinations using Ficoll. Single density equilibrium tubes and density gradient tubes were prepared covering the range of densities equivalent to seawater from 0 to 2000 metres. Trans-Pacific profiles of

salinity at Lat 43°S are available from the Scorpio expedition, and a value of 34.5 °/oo was taken as appropriate at 600-1000 M. Seawater of this salinity will have a density of 1.027 g/cm^3 at 6°C, but an additional correction applies for hydrostatic pressure which increases with depth (e.g. to 1.047g/cm^3 at 4000M).

Most mature orange roughy eggs, both fertilized and unfertilized, sink in seawater at 6°C, but a small proportion (about 10%) float. It is possible, but not proven, that all floating eggs are unfertilized or moribund. Ultrastructural examination can indicate whether this is the case, and samples to explore this possibility have been examined.

Unfertilized eggs taken from ripe (stage 5) females are not uniform in density. In normal seawater some eggs float and others sink, and such eggs equilibrate at different places on a Ficoll column. The condition of the oil droplet within the maturing egg varies, and this variation appears to be related to the egg density. Eggs showing fragmented droplets of oil appear to be less dense and to float . Eggs that sink in seawater can be caused to float in seawater containing 5% Ficoll. Microscopic examination did not indicate any signs of osmotic stress in the eggs, and it appeared that solutions containing up to 5% Ficoll remained close to iso-osmotic.

Equilibration in seawater-ficoll of *in vitro* fertilized eggs and net sample free-spawned (and perhaps fertilized) eggs and developing embryos was explored. It was determined by calculation that the combined effects of salinity, temperature and hydrostatic pressure could be represented at a depth of 200M by 0.98% Ficoll; at a depth of 600M by 2.9% Ficoll and at 1000M by 4.89% Ficoll.

Test tubes containing 1%, 2.5%, 3.5%, or 5% ficoll in seawater were prepared, and fertilized or unfertilized eggs were placed in the upper layer of each tube using a wide bore pipette, approximately 20 eggs per tube. The position of each egg was scored 30 minutes, 12 hours and 24 hours later and recorded as a percentage. Three density categories were recognized in the initial tests, sinking ,floating, or neutral bouyancy. 3.5% ficoll provided neutral bouyancy for the majority of both *in vitro* fertilized and unfertilized eggs. All eggs floated in 5% ficoll. These initial results indicated that newly fertilized or unfertilized eggs should equilibrate between 600 M and 1000M in the watercolumn off St Helens.

Concentrations of Ficoll intermediate between 2.5% and 5%, and prolonged incubations, were included in a later series of experiments, and the overall preliminary conclusion was that newly fertilized eggs should remain at the spawning depth of 600-800M or sink, and should not rise towards the surface .

Net sample free-spawned embryos showing signs of development appeared to equilibrate in 4-5% ficoll suggesting that fertilized eggs dropped from a spawning depth of 600M to 1000M or below during early embryonic development.

4.5 Verification

The above results were transmitted to "Tasmanian Enterprise" (A. Koslow, and T. Davis , CSIRO) and oblique tows using open Bongo nets were extended to a maximum depth of 1200 M. A ring net was also deployed from the "Megisti Star" trawl board to 900M and obliquely towed to the surface. Advanced embryos and a few newly emerged larvae with large residual yolk sacs were obtained in these samples. These embryos and larvae have been filmed on videotape and photographed. Scanning electron microscope images have also been prepared of dissected embryos. (**Figures 4.1- 4.2**)

4.6 Conclusions: 1990-1 work

Ficoll appeared to be suitable for the estimation of egg and embryo density. Some eggs released from spawning females appeared to have a greater bouyancy and to float upwards after spawning. Most eggs and developing embryos had neutral bouyancy equivalent to a water depth of 600-1000 M and should therefore have remained in the spawning water layer or sunk during early development. Limited sampling with open ring or bongo nets confirmed the presence of advanced embryos in samples obtained between 1200M and the surface, but samples of eggs obtained between 600M and the surface contained few advanced embryos and no larvae.

Although the Ficoll experiments carried out in 1990 needed to be repeated, and the net tows needed to be stratified using opening and closing nets, the preliminary results pointed toward a simple physical explanation for the absence of advanced embryos and larvae in surface waters. The work also provided a basis for design of both my own and CSIRO experimental programmes on orange roughy egg development for the 1992 season.

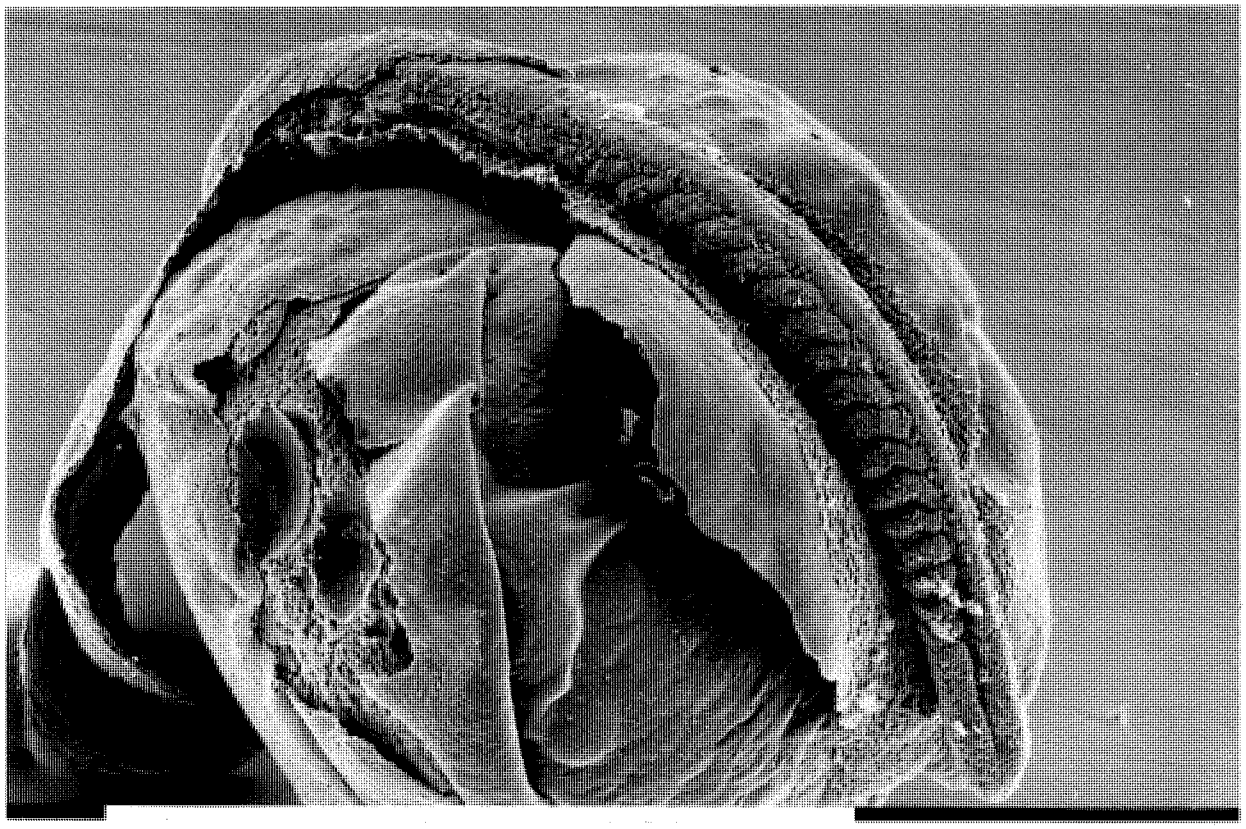

Figure 4.1 SEM of developing orange roughy embryo, dissected from the egg. The trunk somites of the embryo are exposed, lying on the surface of the yolk. Scale bar represents 1 mm.

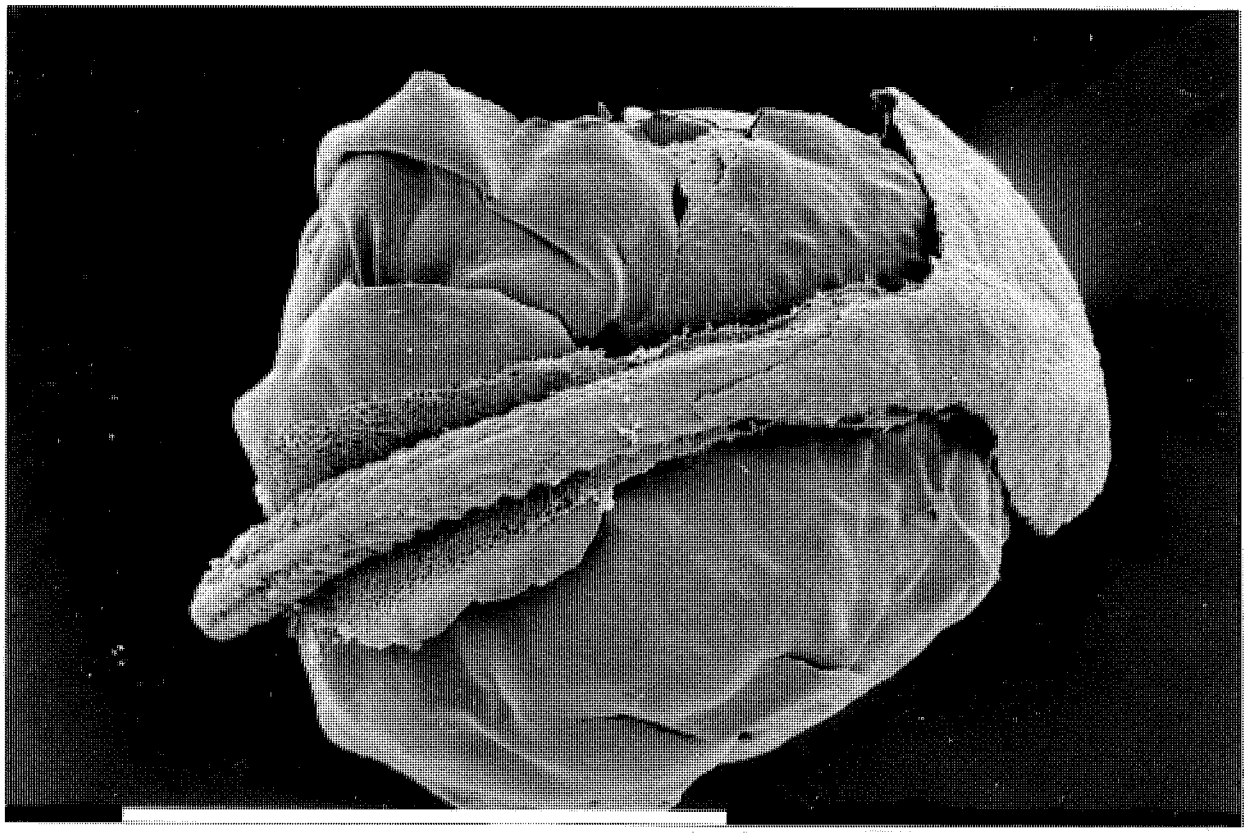

Figure 4.2 SEM of developing orange roughy embryo, dissected from the egg. The posterior somites of the embryo are exposed, but the anterior part of the embryo and head are covered by the amnion, lying on the surface of the yolk. Scale bar represents 1 mm.

5 . Orange Roughy Research 1991-2

5.1 Introduction

My work on orange roughy in the 1991 spawning season included a repeat of the Ficoll density gradient experiments developed in my laboratory to determine the density of roughy eggs and embryos. In 1991-2 experiments were carried out on board the "Southern Surveyor" in collaboration with Dr Koslow, with refined experimental design based on statified plankton survey, using opening and closing nets. Furthermore a more accurate determination of sea water specific gravity was possible using calibrated glass floats. My collaboration was intended to provide indfependent validation for CSIRO egg survey parameters, both in connection with the stratified embryo-larva survey, and in connection with the egg survey protocols.The intention was to predict the dispersal behaviour of embryos from the spawning ground and to indicate where the juveniles might be found. My work was carried out alongside CSIRO programmes supervised by T Koslow and K. Bulman.

5.2 Calibration of Ficoll Density Gradients

Density gradient columns were set up on board the research ship "Southern Surveyor". Columns consisted of rigidly mounted 1000ml cylinders containing 35% seawater with added Ficoll. Columns were constructed with filtered 35% seawater or with synthetic 35% seawater, and gave identical results. Ficoll dilutions in seawater were prepared in shaking flasks and well mixed before introduction into the cylinder. Introduction was through a capillary tube controlled by a valve from a reservoir. (The columns were similar to the stable columns of continuously graded seawater concentration described by Coombs et al 1985). In the 1991 experiments, the density of ficoll-seawater in the column was calculated from published data on ficoll, but in 1992 calibration of the columns was by introduction of calibrated glass floats supplied by The Martin Instrument Co. U.K. The floats are calibrated at 23 degrees Centigrade, but the correction is X 0.000028 for each degree difference in temperature. Experiments to determine the density of orange roughy eggs were performed at 19 C and 6 C, with appropriate corrections applied to float density.

Fig 5.1 shows the relationship between Ficoll concentration and seawater density in one such column(#2)

5.3 Measurement of Density (Specific Gravity) of Orange Roughy Eggs and Embryos.

The density (specific gravity) of orange roughy eggs and embryos was determined using calibrated Ficoll-seawater columns. Eggs and embryos were obtained from orange roughy spawning aggregations at St Helens Hill in three ways :-

a) by stripping unfertilized eggs from running ripe (stage 5) female adults obtained by demersal trawling.

b) by *in vitro* fertilization (IVF) of ripe eggs using sperm from spawning males obtained by demersal trawling. Fertized eggs were maintained on board the research ship in seawater in glass beakers held in the dark at 6 degrees centigrade. The density of developing eggs was measured at 24 hr intervals.

c) by collection from EZ net depth-stratified samples. The EZ apparatus was deployed to allow individual nets to open each 100 metres between 900M and 100M. These samples contained unfertilized eggs, fertilized eggs and early developing embryos.

The density of eggs was determined using calibrated columns (e.g. see **Fig 5.1**), by placing the egg at the top of the column, which contained 34.5 $^{o}/_{oo}$ seawater without ficoll, equivalent in density to the surface water. Most eggs and embryos sank in the column to an initial metastable equilibrium position (termed "entry density"). A second density reading was taken after 8 minutes, at which time most eggs and embryos had reached a stable equilibrium position, reflecting neutral bouyancy in the column. This equilibrium reading was used to determine the equilibrium density. Some eggs and embryos slowly changed their equilibrium density over a period of 48 hrs in the column, presumably as the result of metabolic activity in the embryo (e.g. development, or membrane fluid transfer). **Table 5.1** shows the average density of various egg and embryo sets, (g/cm3).

Unripe and unfertilized eggs from Stage 4 females sink in the column, and have an equilibrium density of 1.0370. This is the density equivalent to seawater 34.5 $^{o}/_{oo}$ at >1000M, and indicates that such eggs would sink to the seabed.

Eggs from running ripe Stage 5 females, unfertilized, mostly have an equilibrium density of 1.0311, equivalent to a neutral bouyancy depth of 400-500M. A small proportion of such eggs are however positively bouyant and float to the top of the density column to an equilibrium density of 1.0235, equivalent to surface seawater at 34.5 $^{o}/_{oo}$

Figure 5.1 Shows the relationship between Ficoll concentration and seawater density in #2 density gradient column. Columns consisted of rigidly mounted 1000ml cylinders containing 35% seawater with added Ficoll. Calibration of the columns was by introduction of glass floats calibrated (with corrections) to maintain neutral bouyancy in the seawater-Ficoll column at19 degrees Centigrade.

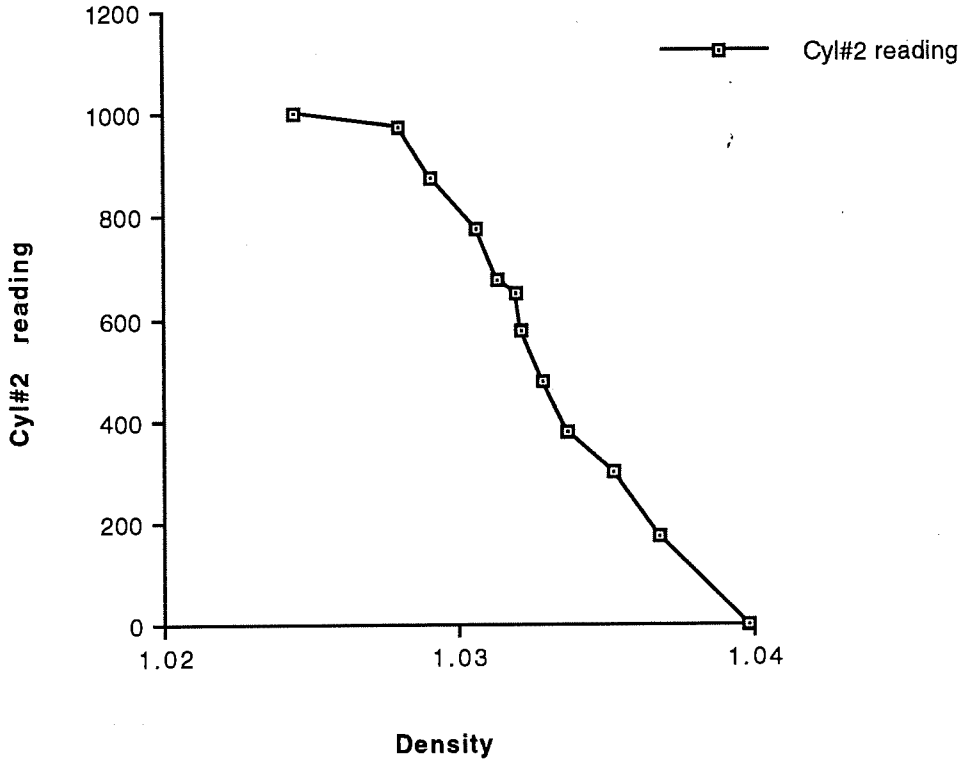

	Egg type	Entry reading	Entry density	Equil. reading	Equil. density	No . of eggs
1	Unri/unfer St4	200	1.0366	150	1.0370	10
2	Unfert.St 5	800	1.0304	700	1.0311	40
3	Unfert.St 5	1000	1.0235	1000	1.0235	5
4						
5	IVF 0 hrs	540	1.0325	720	1.0310	10
6	IVF 24hrs	610	1.0321	720	1.0310	10
7	IVF 34hrs	580	1.0322	600	1.0321	10
8	IVF 52hrs	580	1.0322	600	1.0321	14

Figure 5.2 Density (specific gravity) of the eggs obtained from EZ net samples , as measured in a Ficoll-Seawater density gradient column. Each data point gives the measured average density of 5-10 eggs taken from a single net, open over a range of 100M. The mid point of each oblique tow is taken for each EZ net sample.

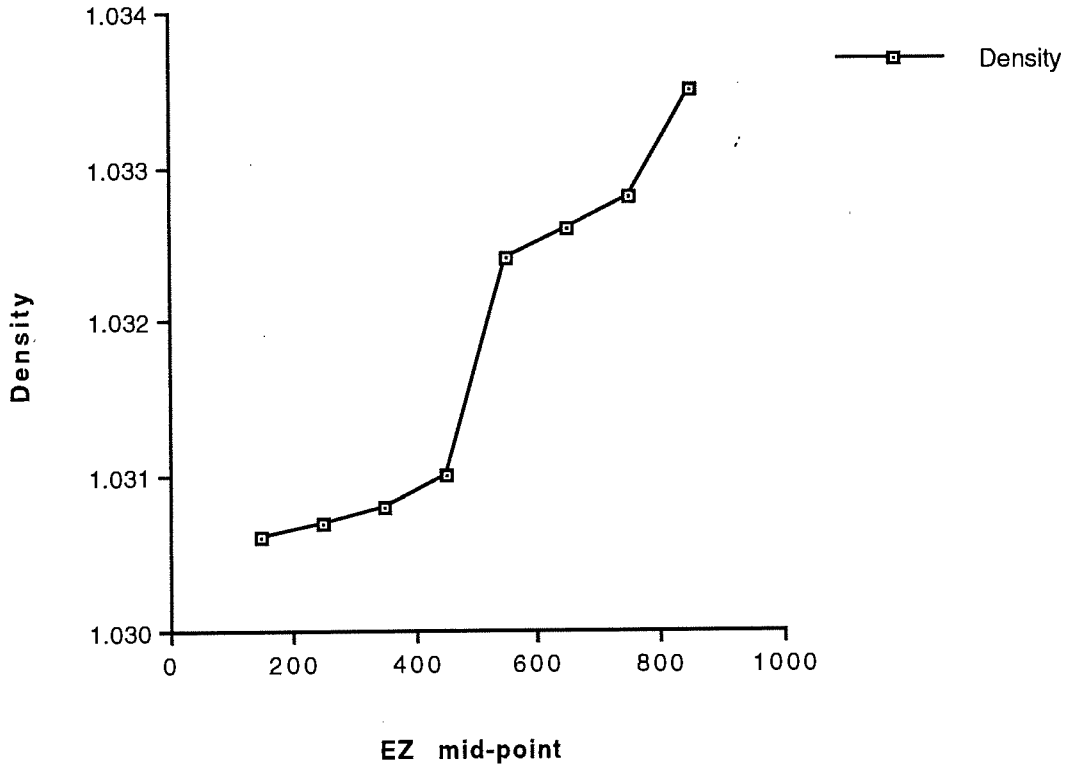

	EZ net	EZ mid-point	Equil. reading	Density
1	EZ 900-800M	850	400	1.0335
2	EZ 800-700M	750	480	1.0328
3	EZ 700-600M	650	500	1.0326
4	EZ 600-500M	550	540	1.0324
5	EZ 500-400M	450	710	1.0310
6	EZ 400-300M	350	755	1.0308
7	EZ 300-200M	250	765	1.0307
8	EZ 200-100M	150	780	1.0306

Eggs fertilized *in vitro* in surface 34.5 $^{o}/_{oo}$ seawater have an initial density of 1.0310, equivalent to neutral bouyancy at about 400M. As these eggs develop, they become more dense, reaching a density of 1.0321 g/cm3 34 hours after fertilization. In terms of neutral bouyancy, this is equivalent to a depth of about 500M.

Eggs and embryos obtained from the water column by EZ net sampling are heterogeneous, with samples containing unfertilized, fertilized and developing eggs. The heterogeneity of the sample is reflected in a wide range of values for the density (specific gravity) of the eggs obtained from a single EZ net sample . Average values obtained are presented as **Table 5.2.** and **Figure 5.2.** Each data point gives the measured average density of 5-10 eggs taken from a single net, open over a range of 100M. The mid point of each oblique tow is taken for each EZ net sample. Two groups of eggs are evident in the sample, a dense group from nets open at 600-900M, and a less dense group taken from nets open 500-100M. Individual samples have been preserved for analysis of fertilization status by microscopy, but this analysis has not yet been completed. Further analysis of the raw data will be required to reveal the reasons for the trends shown in Figure 5.2.

5.5 Microstructure of the Egg and Sperm of the Orange Roughy

The structure of developing, unfertilized and fertilized egg has been studied using the scanning electron microscope in order to establish what changes occur on maturation and fertilization. **Figure 5.3** shows a group of previtellogenic oocytes lying within the ovariole sheath on the surface of a mature oocyte. This preparation was obtained from the ovary of a ripe Stage 5 female. Unfertilized eggs are released with a thin extrachorionic membrane covering the entire egg, which is seen in **Figure 5.4.** The ultrastructure of the chorion in a fertilized egg is well shown in **Figure 5.5** , which shows a torn region of the chorion and the interior of the egg. The outer layer of the chorion bears a spectacular meshwork of reinforcing struts,(see also **Figure 5.6**) whilst the inner layer consists of of compressed lamellae. Pore canals traverse the chorion. **Figures 5.5 and 5.6** are from eggs preserved 48 hours <u>after</u> *in vitro* fertilization, which had led to recognizable pre-gastrulation changes in the embryo blastoderm.

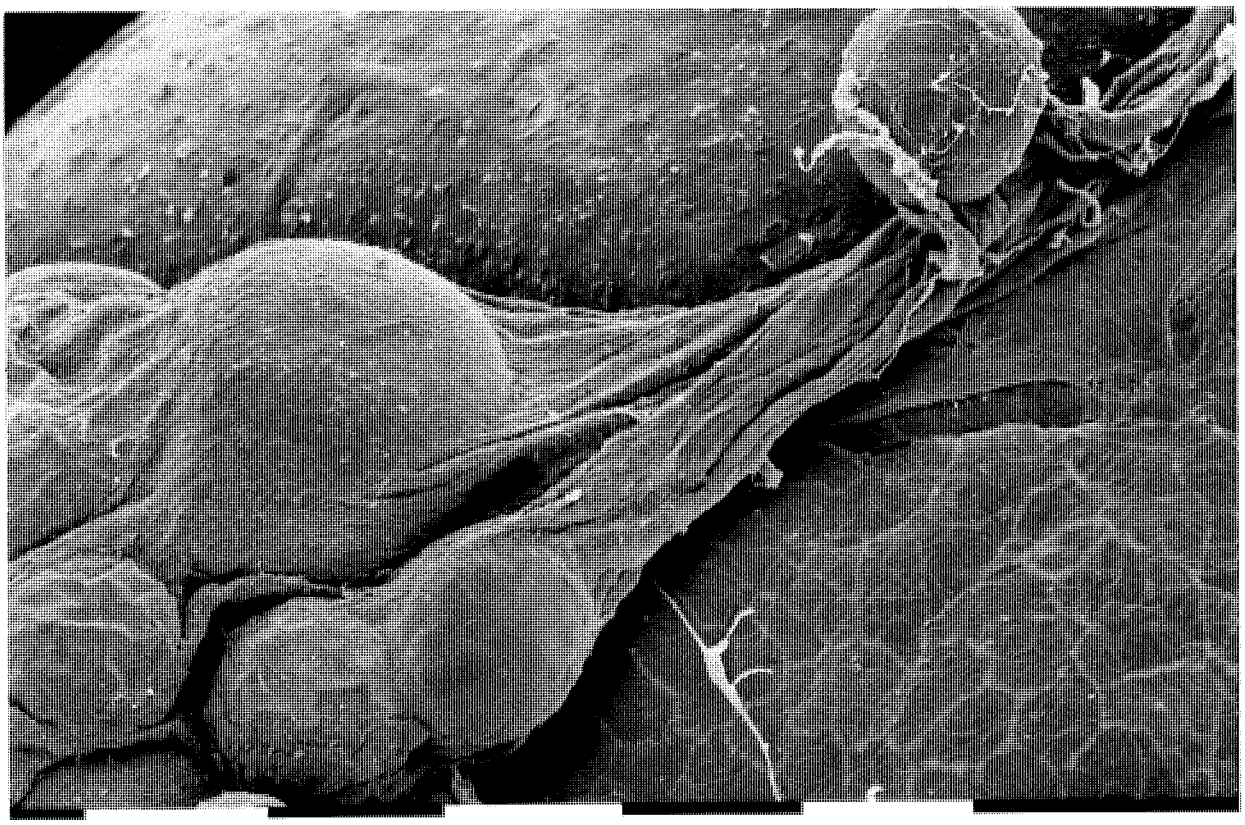

Figure 5.3 shows a group of previtellogenic oocytes lying within the ovariole sheath on the surface of a mature orange roughy oocyte. This preparation was obtained from the ovary of a ripe Stage 5 female. Scale bar represents 0.1mm.

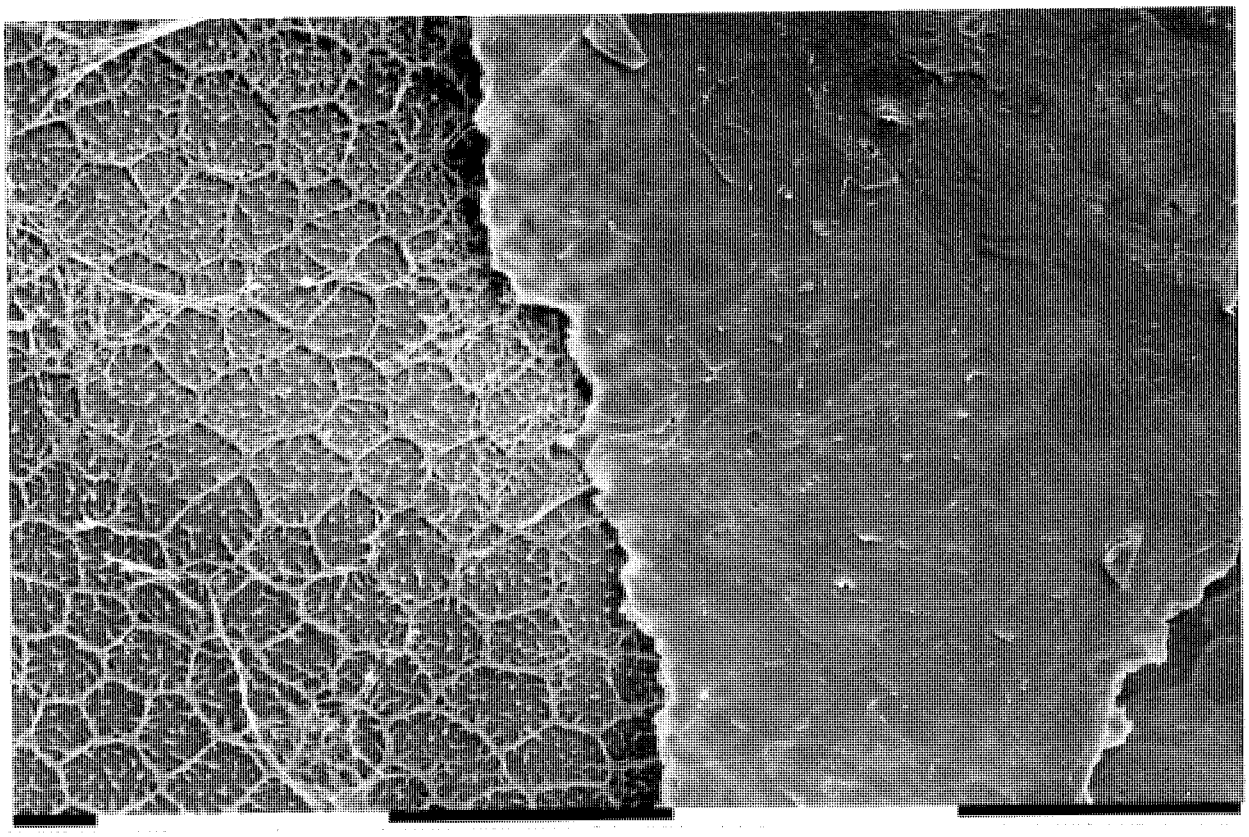

Figure 5.4. Unfertilized eggs are released with a thin extrachorionic membrane covering the entire egg, which is seen here to the right. Scale bar represents 0.1mm.

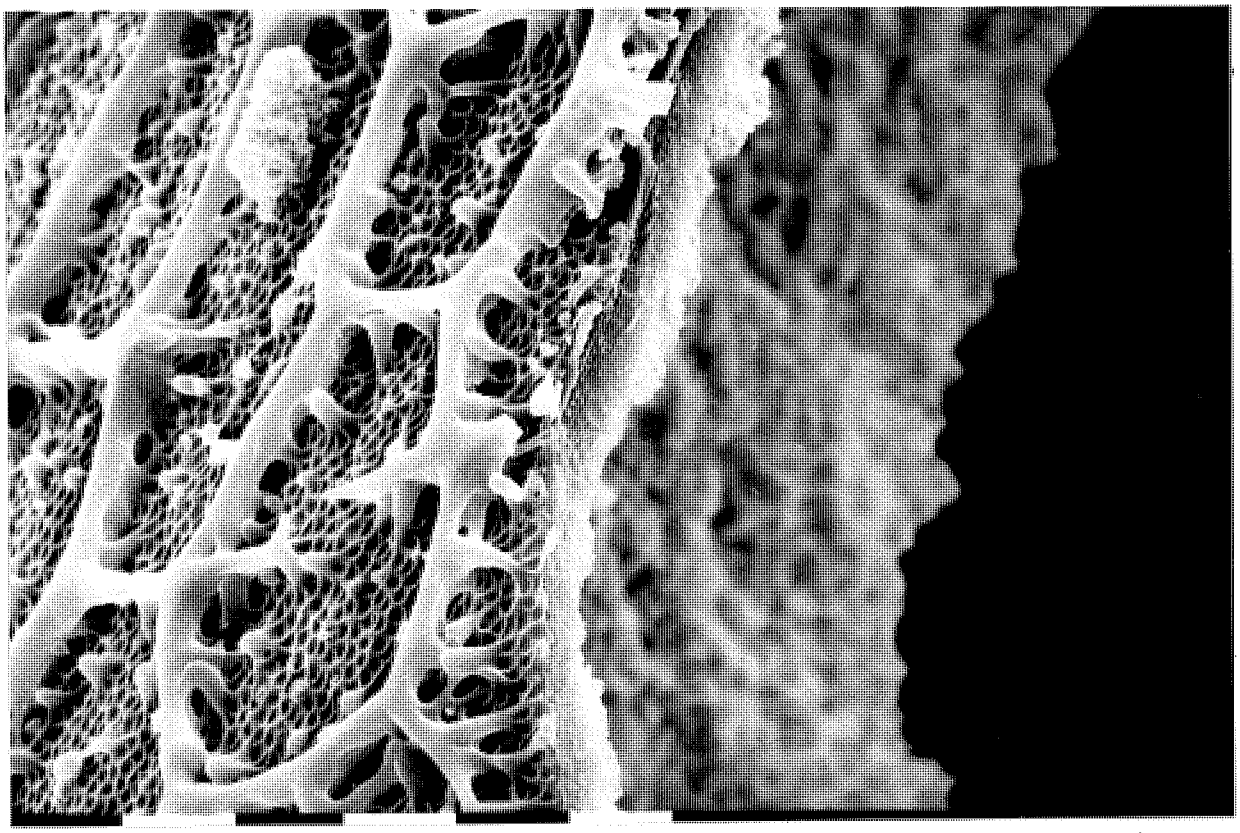

Figure 5.5 Egg preserved 48 hours <u>after</u> *in vitro* fertilization.
The ultrastructure of the chorion in a fertilized egg is well shown in this micrograph , which shows a torn region of the chorion and the interior of the egg. The outer layer of the chorion bears a spectacular meshwork of reinforcing struts, whilst the inner layer consists of compressed lamellae. Pore canals traverse the chorion. Scale bar represents 10 micrometres.

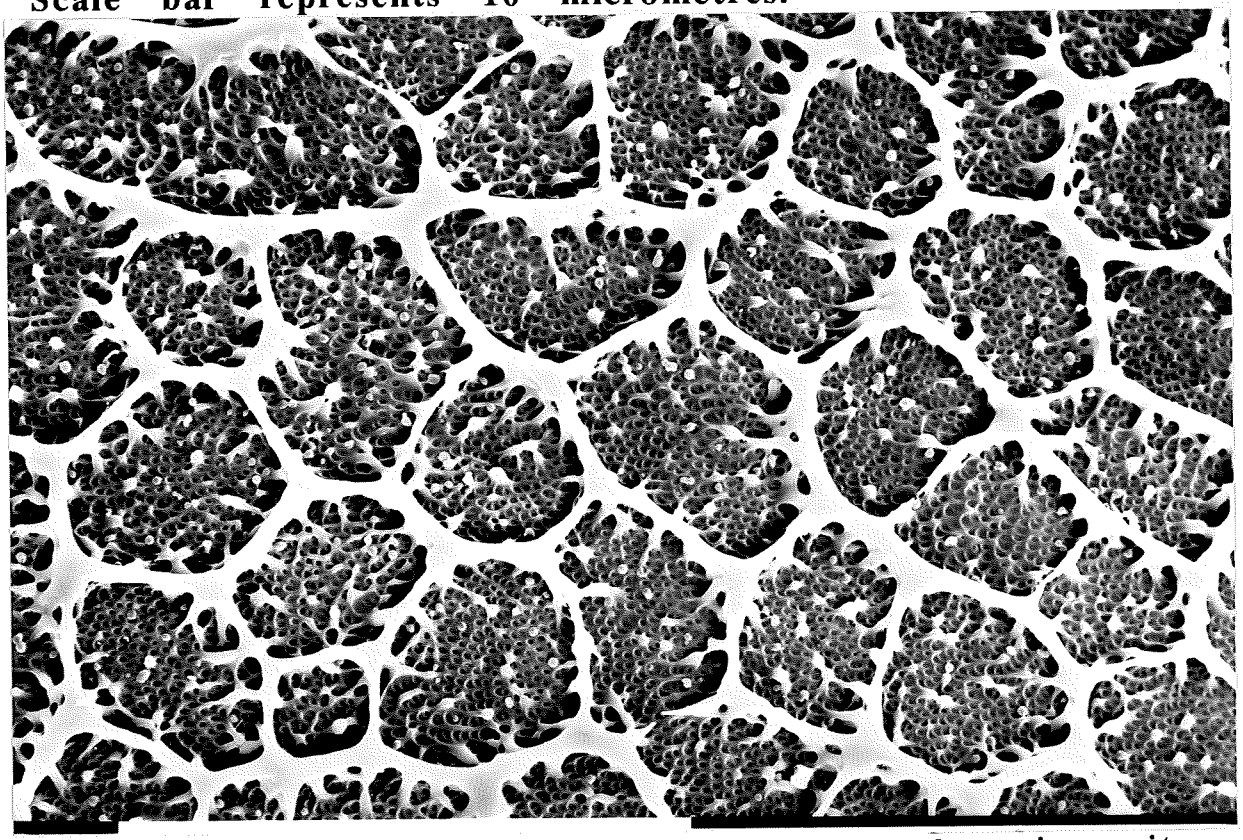

Figure 5.6 Egg preserved 48 hours <u>after</u> *in vitro* fertilization. Surface view of the chorion. Scale bar represents 0.1mm.

The sperm enters the egg through a micropylar apparatus which traverses the chorion. **Figures 5.7 and 5.8** shows the entrance to the micropylar apparatus in a fertilized orange roughy egg. The entrance to the micropyle is about 5 micrometres across, and the vestibule of the micropyle bears a counter-clockwise spiral of reinforcing material.

Examination of the ultrastructure of the orange roughy sperm **Figure 5.9** reveals a stucture well proportioned to make passage through the micropyle. The head of the sperm is pear shaped and is 2.2 micrometres wide. The tail of the sperm is coiled near the tip into a counterclockwise spiral 2.8 micrometres in diameter. The dimensions and pitch aspect of this sperm tail helix should fit neatly into the helix of the micropyle vestibule.

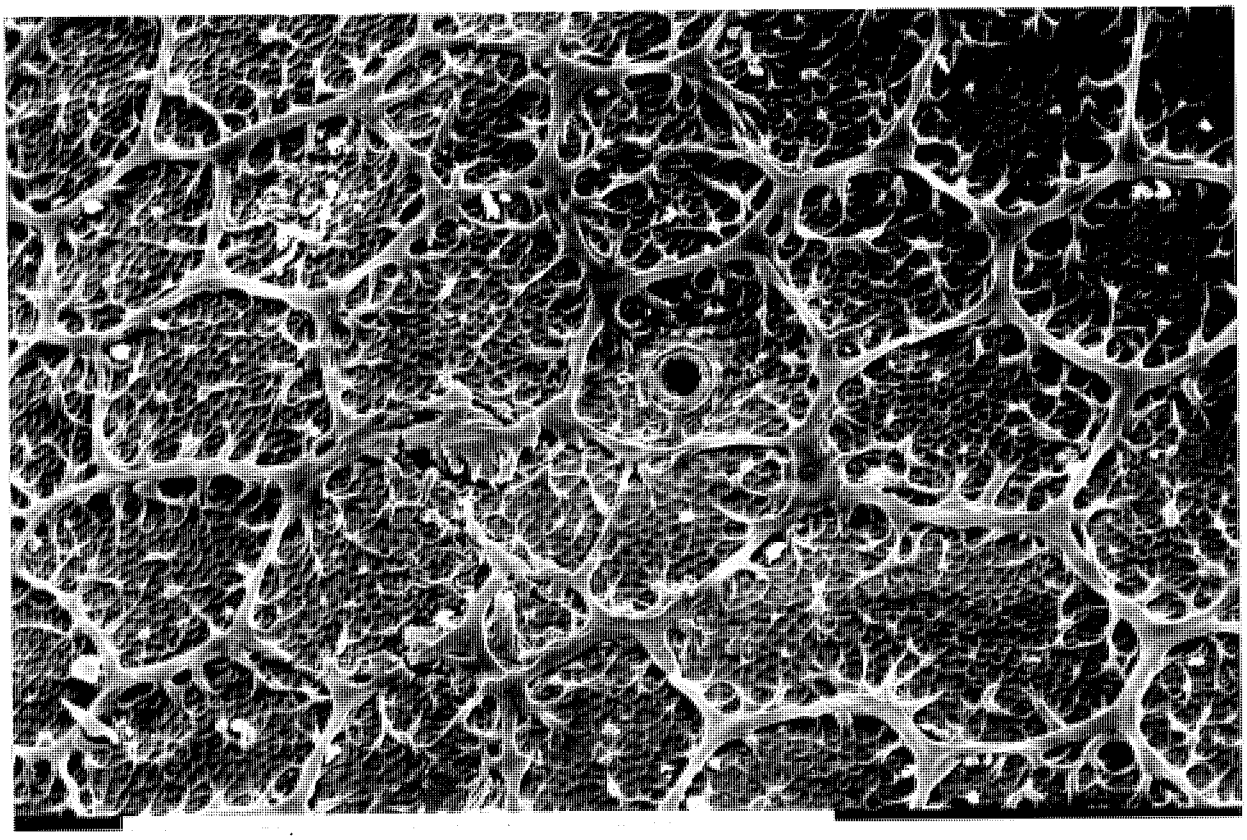

Figure 5.7 Egg preserved 48 hours <u>after</u> *in vitro* fertilization. Surface view of the chorion showing the entrance to the micropylar apparatus. Scale bar represents 0.1mm.

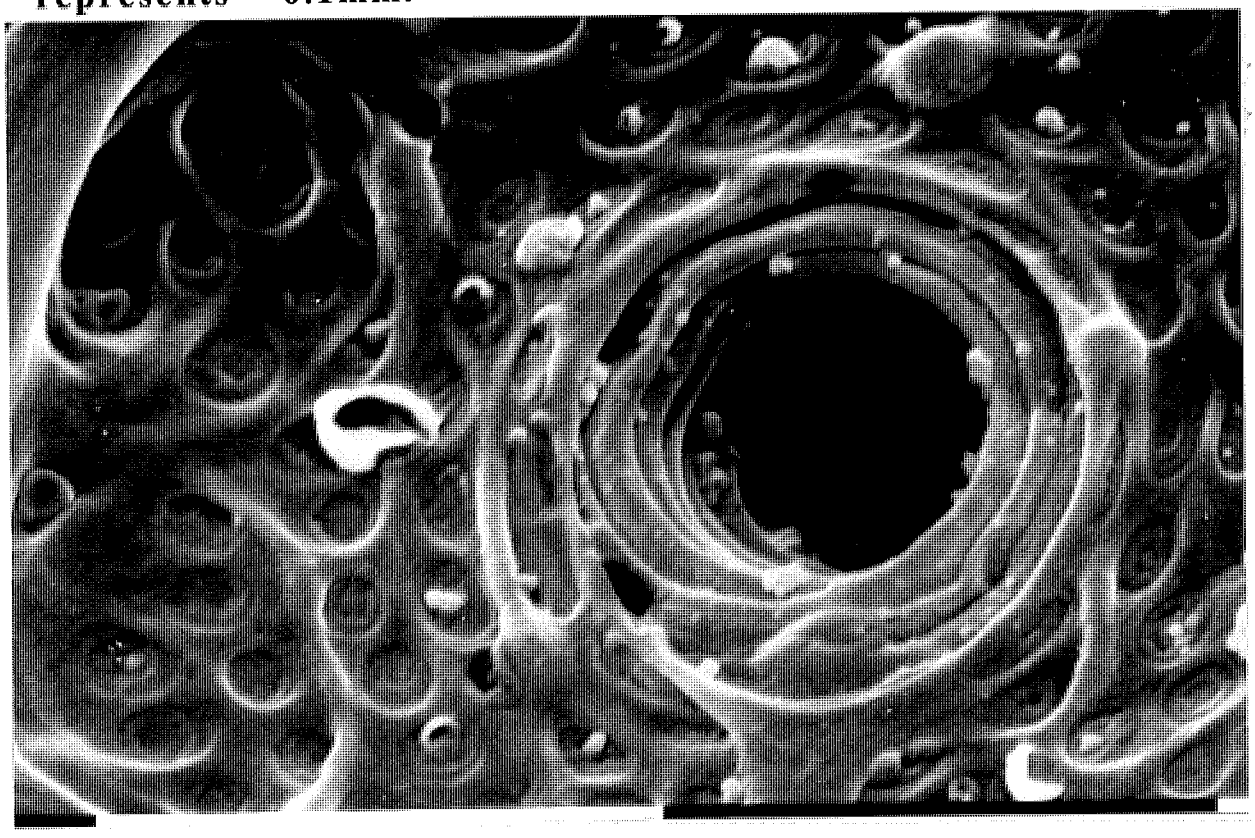

Figure 5.8 shows the entrance to the micropylar apparatus in a fertilized orange roughy egg. The entrance to the micropyle is about 5 micrometres across, and the vestibule of the micropyle bears a counter-clockwise spiral of reinforcing material. Scale bar represents 10 micrometres.

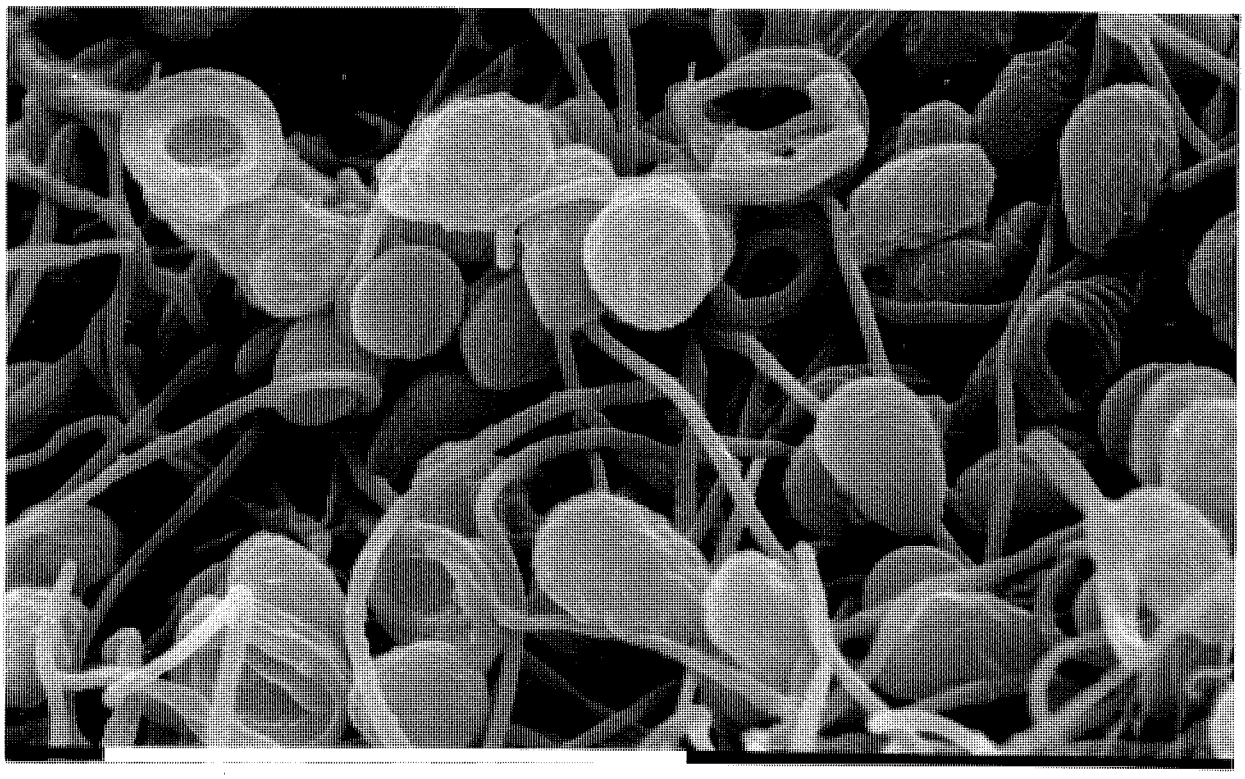

Figure 5.9 Orange roughy sperm from a spawning 38 cm orange roughy. The head of the sperm is pear-shaped and is 2.2 micrometres wide. The tail of the sperm is coiled near the tip into a counterclockwise spiral 2.8 micrometres in diameter. Scale bar represents 10 micrometres.

5.4 Discussion

The factors affecting the vertical distribution of fish eggs have been discussed in a recent paper by Sundby (1991). The spatial distribution of eggs and larvae is a function of the properties of the ambient water (the density, current, and turbulent diffusion) and of the properties of the eggs (the bouyancy and dimension). Study of the vertical distribution is the first step towards understanding the horizontal transport of eggs and larvae. The vertical spreading of bathypelagic eggs such as those of the orange roughy depends mainly on the bouyancy distribution of the eggs.

The specific gravity of the eggs is of primary importance in bouyancy, and the methodology developed in this project enables us to measure the specific gravity of individual eggs, and to use this information to predict the vertical distribution of eggs and embryos. In general neutral bouyancy measurements on living eggs using Ficoll-seawater density gradients corresponded approximately with the observed capture depth by EZ net sampling. It is likely that the Ficoll methodology will replace the conventional use of saline gradients,(e.g. Coombs 1981, Coombs et al 1985, Haug et al 1984) because of the reduced osmotic stress applied to the egg, particularly in columns mimicing a deep water column. The methodology is to be discussed in more detail in a publication in preparation.

The ultrastucture of the orange roughy egg chorion and micropyle are well demonstrated in the present report. Somewhat similar micropylar structures, of different dimensions have been reported in the zebra fish *Brachydanio* (Hart and Donovan 1983). The present work shows the relationship between sperm ultrastucture and micropylar structure in a novel way, and is to form the basis of a publication.

6. Spatial and temporal mapping of age-related changes in orange roughy eye lens crystallins.

6.1 Theory.

Vertebrate eye lens cells contain a number of proteins, collectively called crystallins, that change character during development and ageing. Protein synthesis takes place only in the outer cortex of the lens. As lens cells mature they become part of the lens nucleus and lose the ability to synthesize new crystallins. As a result , the central fibres of the lens contain proteins that are as old as the individual to which the eye belongs, whilst the more superficial fibres contain newly synthesized protein. This feature of lenses has made them ideal for distinguishing age-related changes in proteins occurring during synthesis from those occurring due to post-translational modification. The slow rate of post-translational modifications (when compared to non-lens proteins) reflects the exceptional stability of lens crystallins. Crystallins have been extensively studied in human eye lenses in an attempt to understand this stability, and to work out the causes of pathological conditions, often age-related, such as cataract and presbyopia.

The theoretical basis of the present project was to firstly identify the crystallin-like proteins in the orange roughy lens and map spatial differences (for example between cortex and nucleus), and then to monitor age related changes. Since the lifespan of orange roughies is believed to be equal to, or greater than, the human lifespan, comparable changes might be expected in ageing eye lenses. Differences in the functional properties and operating temperatures of mammalian and fish lenses might be expected to influence the protein changes, and the results of the study are therefore of general theoretical interest towards un understanding of crystallins and ageing.

6.2 Procedures

Using the procedures of high performance liquid chromatography (HPLC), gel electrophoresis in the presence of sodium dodecyl sulphate (SDS), and immunoblotting , it is possible to identify crystallin-like proteins in the orange roughy lens, and compare them with other vertebrate lens crystallins.

Orange roughy eye lenses were obtained by dissection of fresh orange roughy caught at 500-700M off the St Helens Rise, Tasman sea during the CSIRO Southern Surveyor Cruise 3 15/7/92- 28/7/92. The lenses were washed, measured, and then

snap frozen in buffer. On board ship they were maintained at minus 25 degrees centigrade and on shore at minus 70 degrees centigrade, until analyzed.

Paired sets of eye lenses and otoliths were obtained from each fish. Basic biological data, including standard length, weight , and sex were recorded for each fish. Fish ranging in size from 18cm (0.20kg) to 42 cm (1.92kg) were included in the sample.

Analysis involved initial dissection of the thawed lens to remove the capsule, and separation of the cortex and hard central nucleus. Each component was separately homogenized in buffer, centrifuged and washed, and pellets were resuspended in SDS. The protein concentration of homogenates was determined spectrophotometrically. Polyacrylamide gel electrophoresis was performed in the presence of SDS (SDS-PAGE), and protein subunits visualized by Coomassie blue staining.

Gel filtration was performed on a Superose FPLC column (Pharmacia 12HR 10/30) The samples were eluted from the column with Tris buffer and the absorbance of the protein was monitored at 280 nm. The major peaks were collected and analyzed by SDS-PAGE and Western Blots.

Immunochemistry Orange roughy lens proteins were analyzed for cross-reactivity with polyclonal antibodies made in rabbit to bovine crystallins by a Western Blot procedure. Five types of antibody against bovine crystallins were available. (i) An antibody to total Gamma crystallins; (ii) An antibody to Alpha A crystallins; (iii) An antibody to Alpha B crystallins; (iv) An antibody to Beta crystallins; (v) An antibody to high molecular mass Beta crystallins. Protein was electroblotted onto nitrocellulose paper and probed with these four types of antibodies.

Flow diagram

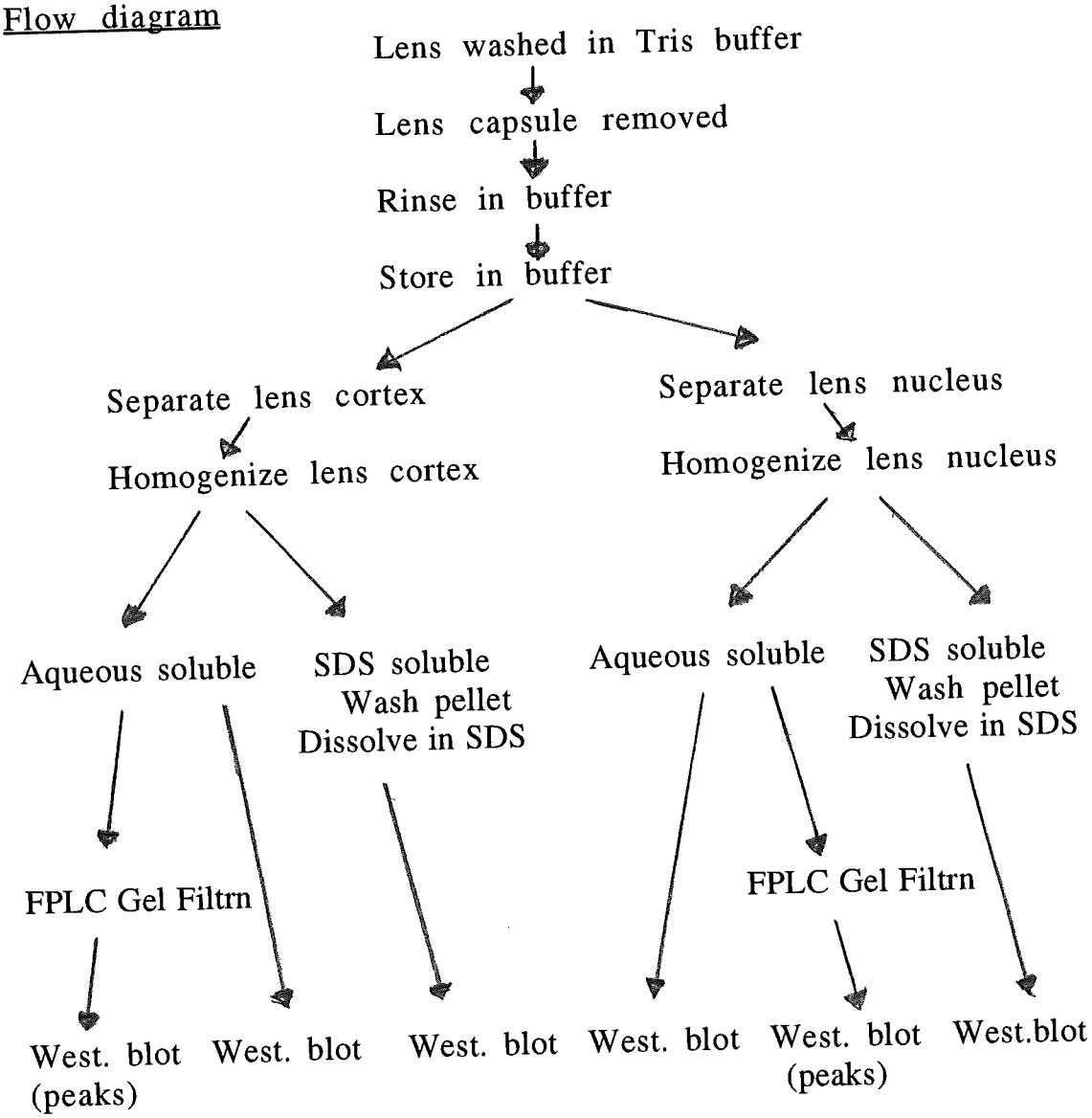

6.3 Results Summary

6.3.1 Percent Aqueous Soluble Protein (by wet Weight)

The proportion of aqueous soluble protein in the lens for fishes of different standard length is shown in **Figure 6.1**. The data refers to a known sample weight for each lens. The cortex contains on average 42.6% soluble protein, whilst the nucleus contains on average 12.1% soluble protein. This means that the nucleus has approximately 28% of the soluble protein contained in the cortex. (See also Section 6.3.5).

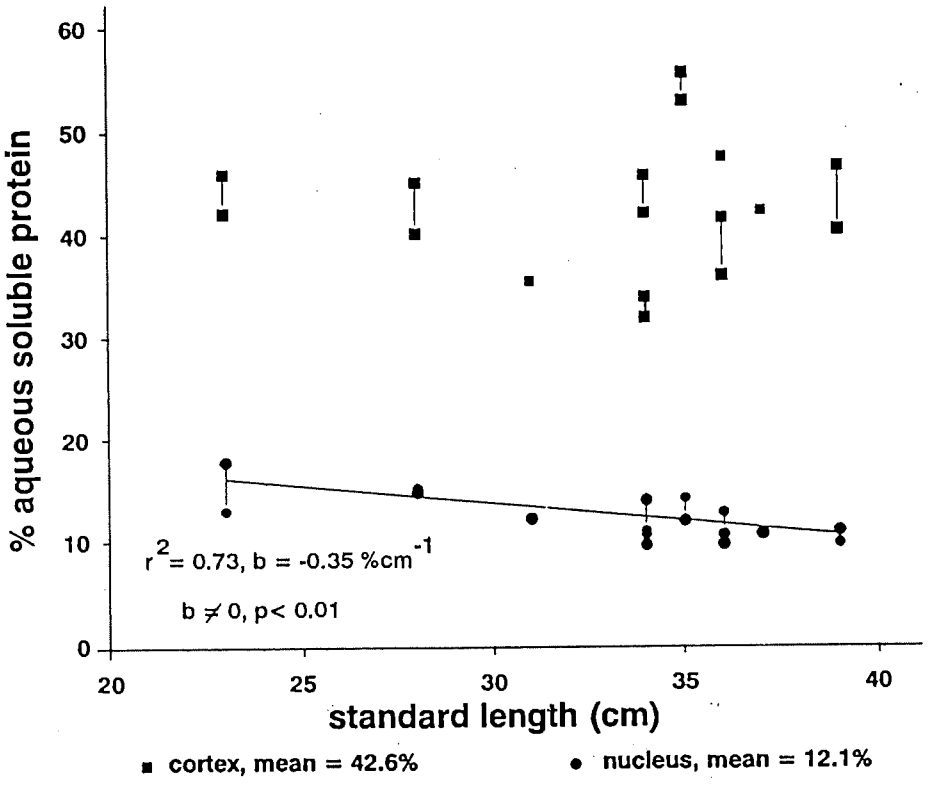

Figure 6.1 Percent Aqueous Soluble Protein in Lens. Vertical bars connecting points indicate that the lenses were taken from the same fish.

6.3.2 Gel filtration

Orange roughy lens cortex proteins resolve as seven peaks by FPLC gel filtration (Figure 6.2) :

Peak #1	>2000 kD
Peak #2	589 kD
Peak #3	199 kD
Peak #4	63 kD
Peak #5	37 kD
Peak #6	19 kD
Peak #7	15 kD

The orange roughy nuclear proteins are contained within peaks #1, #4 +#5, and #6 + #7. Peaks #2 and #3 are insignificant in the nucleus.

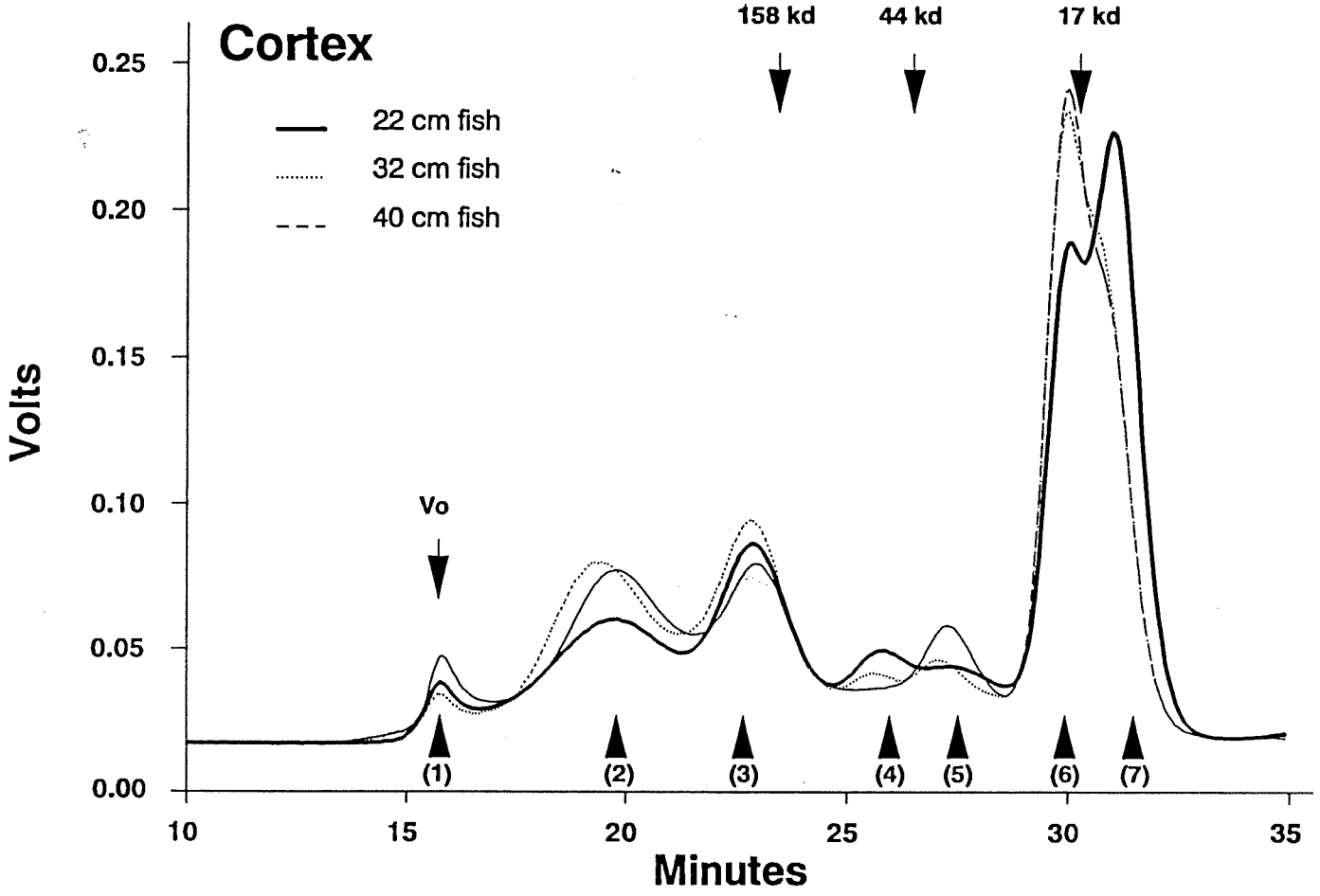

Figure 6.2 FPLC Gel Filtration of Lens Cortex
Data for 22, 32, and 40 cm fish is shown, and approximate molecular weights for major peaks #3-#7 are indicated.

6.3.3 Antigenic relationships

The antigenic relationship of orange roughy lens proteins to bovine lens proteins was investigated using polyclonal antibodies made in rabbit to bovine crystallins by a Western Blot procedure. Orange roughy protein was electroblotted onto nitrocellulose paper and probed with five types of antibodies against bovine crystallins. Peaks #4 and #5 showed strong cross reactivity with rabbit antibodies (iv and v) against bovine Beta crystallins, and high molecular mass Beta crystallins. Peaks #6 and #7 showed strong cross reactivity with rabbit antibodies (i) against total Gamma crystallins. None of the orange roughy elution peaks, nor the void volume peak #1, showed any cross reactivity to antibodies (ii) and (iii) to Alpha crystallins.

A comparison of aqueous soluble fraction and SDS-soluble fractions of both the nucleus and cortex of the lens are shown in **Figure 6.0** The data show that peaks #6 and #7 are Gamma crystallins. Approximately 85% of the nuclear aqueous soluble protein elutes in peaks #6 and #7 (Table 6.1). SDS-PAGE (**Fig 6.0a, lanes 1,9**) shows that the major proteins of the lens nucleus have subunit molecular masses of approximately 20kD, and these subunits cross react with antibodies made to bovine Gamma crystallin (**Figure 6.0b ,lanes 1,9**). The data also show that Beta crystallin occurs in some or all of the remaining peaks which make up approximately 52% (Table 6.1) of the cortical aqueous soluble protein. SDS-PAGE reveals that the cortex contains proteins with subunit molecular mass ranging from approximately 35kD to approximately 25kD (**Fig 6.0c,lane 5**). These bands cross react with antibodies made to bovine Beta crystallin (**Figure 6.0 d,e, lane 5**) We found that antibodies made to bovine alpha crystallin do not cross react with proteins in orange roughy lenses (data not shown here). Western blot analysis of the FPLC peaks will provide a clearer picture of the proteins contained in each of the peaks

The data show that the SDS-soluble fraction of the nucleus (NI) has Beta crystallin bands that are more or less absent from the aqueous soluble fraction of the nucleus (N) which is almost solely composed of Gamma crystallin (**Figure 6.0**) The SDS -soluble (CI) and aqueous soluble (C) fractions of the cortex have approximately the same amount of beta crystallins, though the subunit molecular weights of these beta crystallins is not always the same. The higher molecular weight proteins in CI are presumably cytoskeletal proteins such as actin.

Figure 6.0 shows a comparison of aqueous soluble fractions and SDS-soluble fractions of both the nucleus and cortex of the lens.

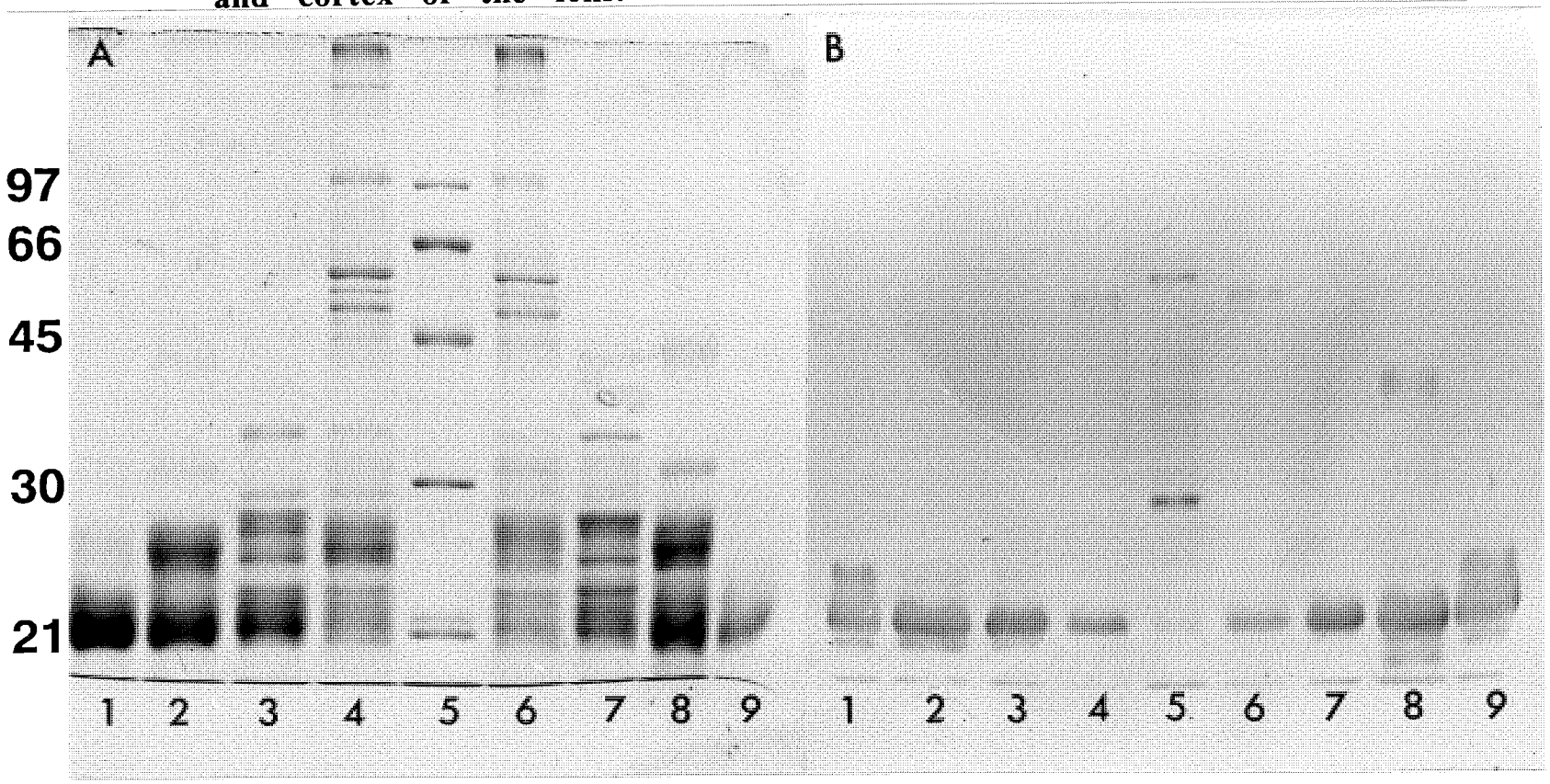

(**a**) Gel of a 23cm female and 39cm male orange roughy.
(**b**) Western blot of (**a**) with bovine anti Gamma crystallin: 1a=1b=aqueous soluble nucleus (N) of 23 cm female; 2a=2b= SDS soluble nucleus (NI) of 23 cm female; 3a=3b= aqueous soluble cortex (C) of 23 cm fish; 4a=4b= SDS soluble cortex (C) of 23 cm fish; 5a=5b= standard; 6a=6b= CI of39 cm fish; 78a=7b= C of 39 cm fish; 8a=8b= NI of 39 cm fish.

Figure 6.0 shows a comparison of aqueous soluble fractions and SDS-soluble fractions of both the nucleus and cortex of the lens.

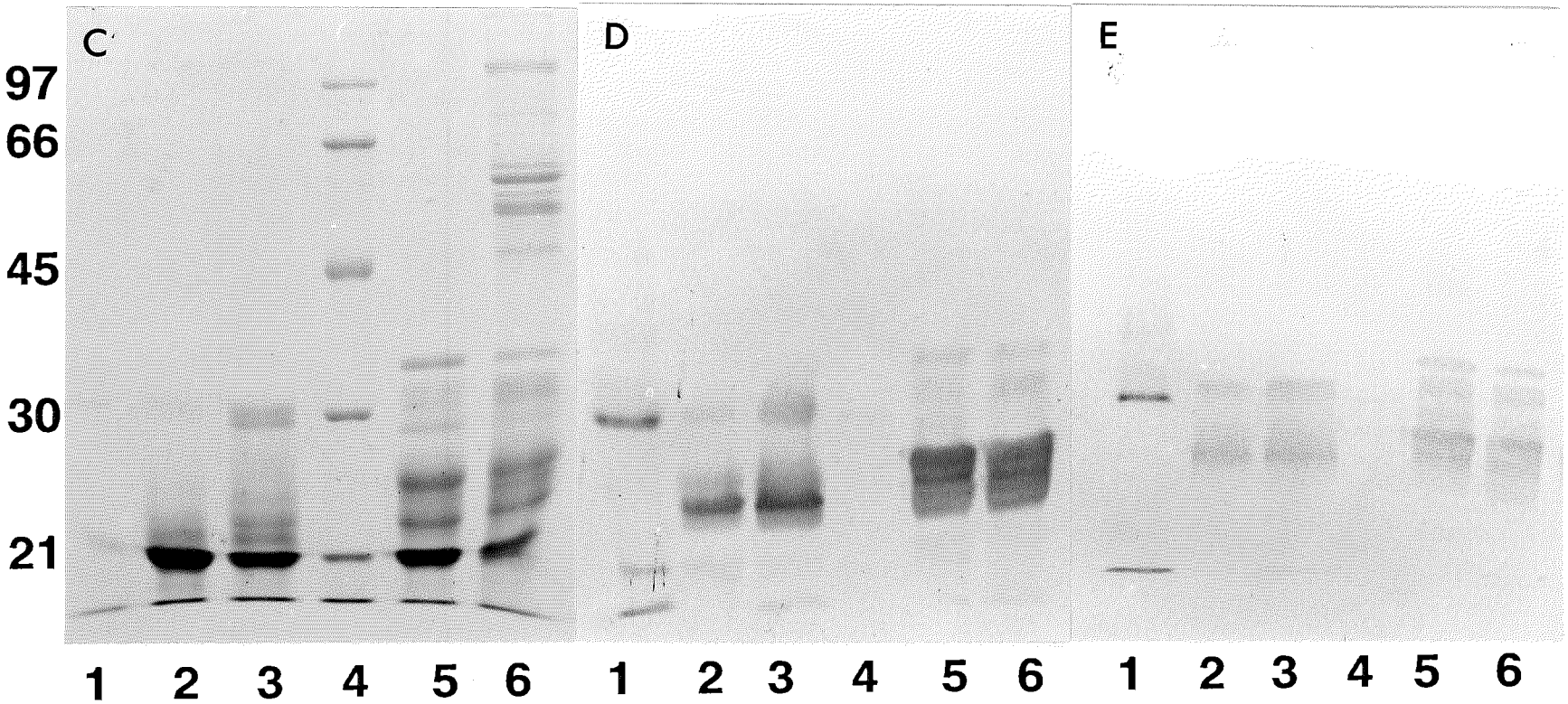

(**c**) gel of 37 cm female
(**d**) Western blot of (c) with bovine anti-Beta crystallin.
(**e**) Western blot of (c) with bovine anti-betaH-crystallin.
1 (a,b,c)= biotinylated standards, 2 (a,b,c) = N, 3 (a,b,c,)= NI, 4 (a,b,c) = standards, 5 (a,b,c) = C, 6 (a,b,c) = CI.

The elution profile of the orange roughy lens is analagous to the human lens (McFall-Ngai et al.1985). In young human lenses Alpha crystallin elutes out in the void volume containing proteins of molecular weight greater than 350kD and by analogy orange roughy Alpha crystallin would form part of peak #1. Human Beta crystallins appear as several peaks of about 45kD, and by analogy orange roughy Beta crystallins would form peaks #4 or#5. Human Gamma crystallins of molecular weight 19-21kD elute together, and by analogy orange roughy Gamma crystallins would form peaks #6 and #7.

6.3.4 Post-Translational Modification of Crystallins.

The resilience of different peaks to post-translational modification is indicated by the analysis given in **Table 6.1**, which compares the peaks in the nucleus and cortex. Peak #2 and#3 in the nucleus occupy only 2.5% and 3% of the area they occupy in the cortex, whereas peaks #6 + #7 in the nucleus occupies 50% of the area they occupy in the cortex.

	X = Cortex, % of total area	Y = Nucleus, % of total area	% cortical protein remaining in nuleus =((Y/3.5)/ X) x 100	% of total soluble protein = (X+(Y/3.5))/128) x 100
Peak 1	2.5	2.0	22.8	2.8
Peak 2	19.7	1.7	2.5	15.8
Peak 3	19.8	2.1	3.0	15.9
Peak 4 + 5	8.7	10.7	36.5	6.0
Peak 6 + 7	48.1	85.0	50.5	56

Table 6.1 Post-Translational Modification of Crystallins.

Unfortunately lenses from small juvenile orange roughies (below 18 cm standard length) were not available, so it was not possible to determine how much change had already occurred in the smallest fishes available to us. If the juvenile cortical pattern is substantially similar to the pattern of 18+ cm fish, then we can say that the crystallins of peaks #2 and #3 (Beta and Alpha crystallins) are more susceptible to post translational modification than are peaks #6 and #7 (Gamma crystallins).

6.3.5 What are the changes in synthesis with age?

In the Cortex, significant changes occur in peaks #5,6, and 7 between 22cm and 40 cm fish as shown in **Figure 6.2,** in which chromatograms of the lens cortex are overlayed. The 37kD peak #5 and the 19kD peak #6 become significantly larger with ageing, whereas the 15kD peak #7 becomes smaller. This represents a significant change in the synthesis of monomeric Gamma crystallins appearing as peaks #6 and #7.*(Decrease in peak #7 : slope = -1.5%cm^{-1}. 95% confidence interval of slope b = (-1.34,-1.70 5 cm^{-1}), b = 0 for p< 0.01).*
(Where distinguishable, the increase in peak #6 : slope = -1.0 %cm^{-1}, 95%confidence interval of slope b = (0.85, 1.07 %cm^{-1}), b=0 for p< 0.01).The overall decrease in peaks #6 +#7: slope = 0.5 %cm^{-1}, 95% confidence interval of slope b = (0.44,-0.53 cm^{-1}), b=0 for p< 0.01). When the ratio of the area of peak #5 to the total area of all peaks is plotted against standard length of the fish, a linear increase is noted **(Figure 6.3)**. This increase indicates that either changes in levels of protein synthesis, or post-translational changes, are occurring in the proteins represented by this peak.*(Increase in peak #5: slope = 0.3 %cm^{-1}, 95% confidence interval of slope b = (0.29, 0.32 cm^{-1}), b= 0 for p<0.01).*
No significant trends were found to hold in the remaining peaks.

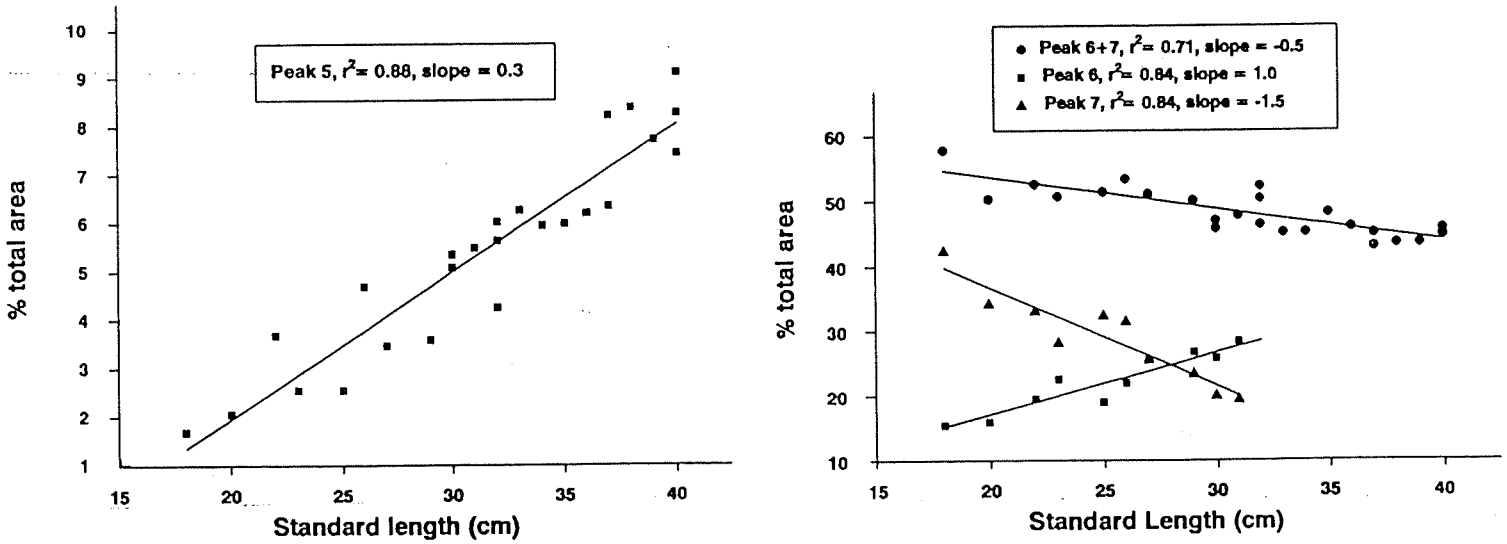

Figure 6.3 Changes in Cortex proteins with Age.
The ratio of the area of peaks #5,6,&7 to the total area of all peaks is plotted against the standard length of the fish. Changes indicate ageing of lens proteins

In the lens nucleus, Peaks #1,5, 6 and 7 can also be resolved in some preparations, and the same trends occur in peaks #5, 6 and 7 (Figure 6.4) (i.e the 37kD peak #5 and the 19kD peak #6 become larger with ageing, whereas the 15kD peak #7 becomes smaller).

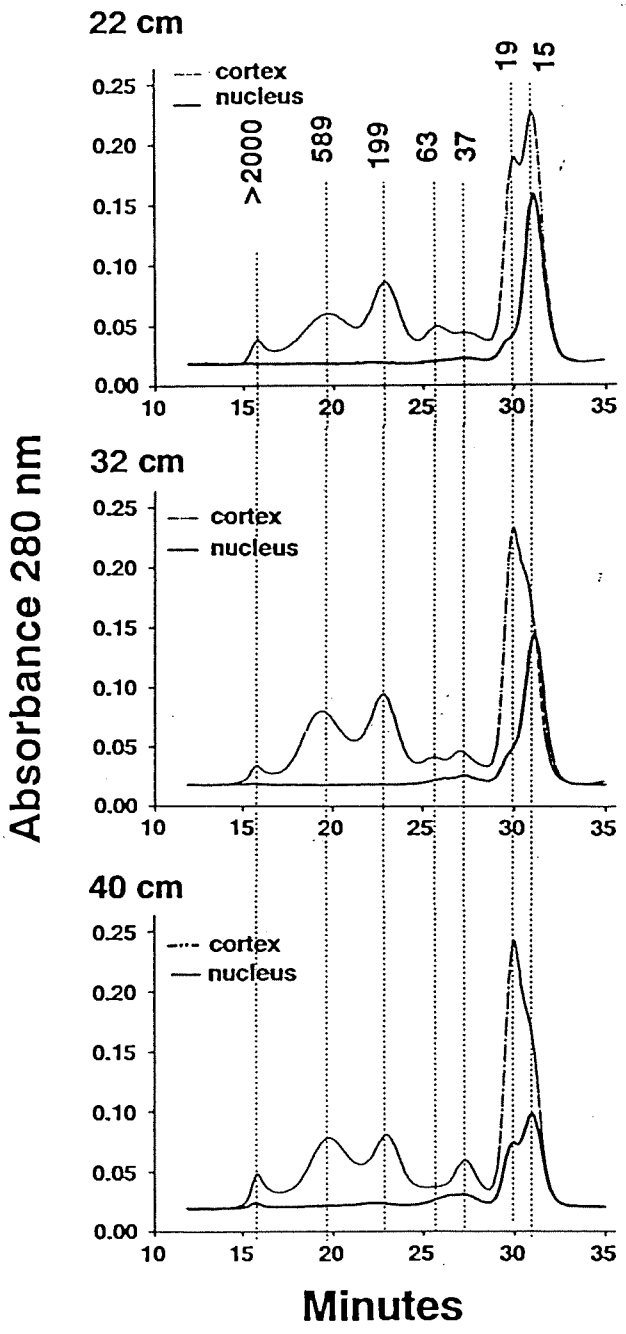

Figure 6.4 Changes in Lens proteins of nucleus and cortex with age. FPLC Data for 22,32, and 40 cm long fish.

In the cortex very similar changes occur , with a nearly linear decline in peak #7 (**Figure 6.3**) , and a strong increase in peak #5 (**Figure 6.3**).

The proportion of aqueous soluble protein in the nucleus and cortex has been determined (**Figure 6.1**) . The nucleus has about one third less aqueous soluble protein than the cortex. During ageing from 18cm length to 40 cm length small decreases in aqueous soluble proteins within the nucleus are revealed (**Figure 6.1**). *(% soluble protein of nucleus b = -0.35, b = 0 for p<0.01, mean 12.1%).*

Significant changes in the areas of FPLC protein peaks occur during ageing of the orange roughy indicating that post-translational changes are occurring. **Figure 6.4** shows a comparison of chromatograms of cortex and nucleus.

In the nucleus there is a nearly linear decline in the combined areas of peaks #6 + #7 (Gamma crystallins) relative to the total area (**Figure 6.6**). This decline is the result of a strong reduction in the area of peak #7 (**Figure 6.7**). Both changes are nearly linear in fishes from 18cm to 40 cm in standard length. *(Decrease in #6+#7 in the nucleus : slope = -1.2 5cm^{-1}, 95% confidence interval of slope b = (-1.03, -1.35 5cm^{-1}),b=0 for p, 0.01).* Peaks #6 and #7 are distinguishable for fish >38cm, and qualitatively it appears that ratio 6:7 increases with the standard length of the fish, reflecting presumably an increased ratio with age.

During the same period of the life history there is a marked increase in the area of peaks #4 and #5 (Beta -crystallins) in the nucleus (**Figures 6.6 and 6.7**). *(increase in #4+#5: slope = 0.6%cm^{-1}*

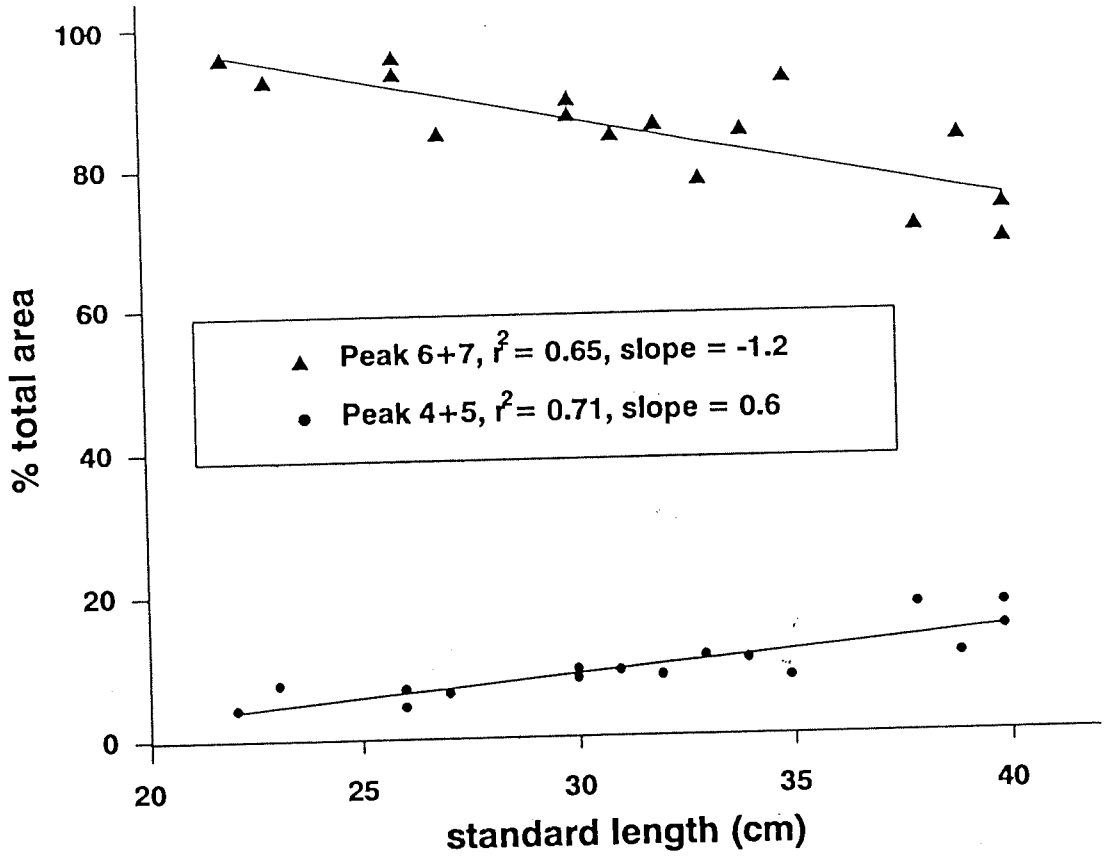

Figure 6.6 Changes in Lens Nucleus proteins with fish length

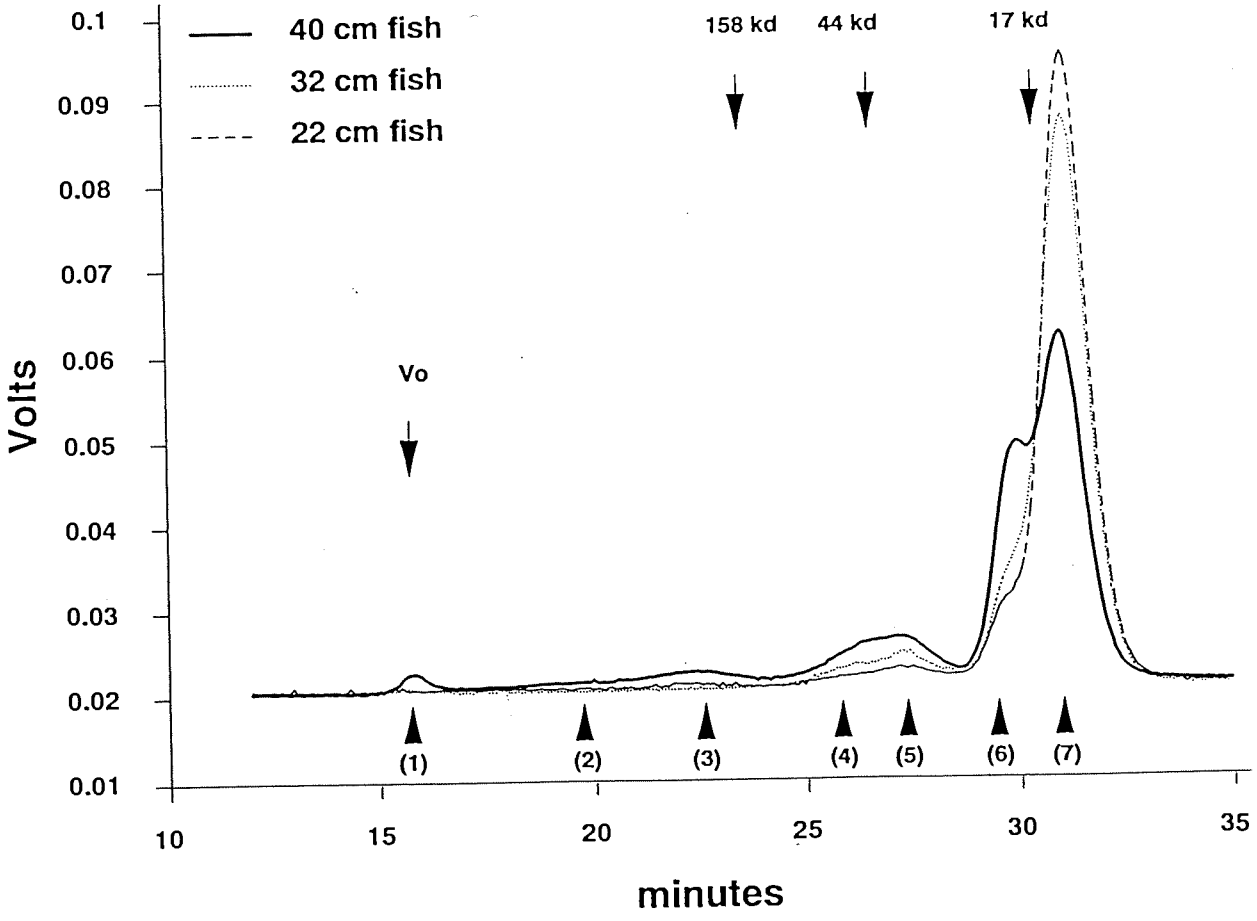

Figure 6.6 Changes in Lens Nucleus proteins with fish length

6.4 Discussion

Most studies on the effects of ageing on lens crystallins have been on terrestrial vertebrates, perhaps because of the ease with which age can be determined, and of course because of the central preoccupation with human ageing processes.

The Orange Roughy teleost fish (*Hoplostethus atlanticus* Trachichthyidae) has a lifespan variously estimated between 80 and 140 years, depending on the ageing technique used. Reproductive maturity appears to be reached at about 32 cm body length, at an estimated age of approximately 30 years (Fenton et al. 1991). This represents an average growth rate of approximately 1 cm per year.

The adult Orange Roughy is caught is caught at depths of 500-800 metres, where the temperature remains close to 6^0C, and the only light is that produced by bioluminescent organisms. This constitutes a fairly stable environment in comparison to that experienced by most vertebrates with comparable lifespans, especially human beings. Thus the confounding effects of a varying environment on lens proteins are minimized, allowing a more accurate determination of the effects of time (i.e. ageing) on these proteins.

Our study shows that there are several important differences in the protein composition of mammalian lenses and orange roughy lenses. The orange roughy has an exceptionally high proportion of gamma crystallin: 48% of the cortical proteins, and 85% of the nuclear proteins. (56% total aqueous soluble protein. A recent review (de Jong et al, 1989) places an upper level of 40 % on the amount of gamma crystallins to be found in all vertebrates. Furthermore the crystallins with a native molecular weight greater than 350kd do not cross-react with bovine anti alpha or rat anti alpha antibodies, even though bovine anti alpha antibodies have been shown to cross-react with crystallins with similar native molecular weight found in other

deep sea teleosts. (McFall-Ngai et al 1986). This fact suggests that Orange Roughy alpha crystallin may be considerably different from mammalian alpha crystallin.

Recently, bovine alpha crystallin has been identified as a molecular chaperone (Horwitz 1992), binding to other crystallins, and preventing the formation of high molecular weight aggregates, thus slowing the rate of insolubilization of these proteins. Given the suggested difference between bovine and

Orange Roughy alpha crystallin, it would be interesting to determine whether the fish alpha crystallin is a molecular chaperone.

The percentage of aqueous soluble protein in the lens cortex of the Orange Roughy remains constant as the fish grows, as reflected by increasing length and otolith weight, though the percentage of aqueous soluble protein in the lens nucleus decreases with standard length. These results are consistent with the idea that protein synthesis continues at a constant rate in the cortex, but does not occur at all in the nucleus. In the human eye lens there is a decrease in the rate of protein synthesis with age (Mc Fall-Ngai et al, 1985), but this difference may be explained by the determinate growth of humans, in contrast to the indeterminate growth of fishes. As our data begins with fish already 18 cm long, and probably 20 or more years old, there may have already been a n earlier decline in protein synthesis.

Although there is no detectable change in the overall rate of synthesis of total lens protein, there are changes in the rates of synthesis of individual proteins, and even detectable changes within crystallin species. There is an overall decline in gamma crystallin synthesis (peaks #6 + #7), as a result of the downturn in the synthesis of the protein of peak#7, and a lesser increase in the synthesis of peak #6. A decrease in the rate of synthesis of lower molecular weight gamma crystallin (combined 19 kD and 21 kD) with age has also been detected in the human lens (McFall-Ngai et al 1985; Zigler et al 1985), though an increase in the synthesis of the higher molecular weight gamma crystallins (23kD) has not been detected. The cause of the relative increase of peak #5 with increasing length has yet to be assessed.

The hard fibrous centre of the lens, termed the nucleus, is made up of the embryonic nucleus and adult nucleus combined. It increases in size with age as older cortical fibres become part of the nucleus. This feature of fish lens nuclei implies that they will contain a record of the changes in synthesis that have taken place in the cortical fibres. It is thus not surprising that we detect a qualitative increase in the gamma crystallin peak #6 with age.

Quantitative analysis is is limited by the fact that peaks #6 and #7 are only distinguishable for fish greater than 38cm. There is a similar increase in the proteins of peaks #4 + #5.

Several possible explanations can be advanced for the large amount of gamma crystallins found in the nucleus of younger fish (18-26 cm). One possibility is that gamma crystallin is the only crystallin species synthesized in embryonic or newly hatched fish. Another possibility is that Orange Roughy gamma crystallin

is more resistant to post translational modifications than other crystallins. The definitive method to resolve this dilemma would be to examine the chromatograms of newly hatched or embryonic fish, but this material was not available at the time of the study. An alternative is to examine the nucleus of the 18 cm fish and attempt to determine the nature of the post-translational modificationsthat we know have occurred due to the decrease in percentage aqueous soluble protein in the nucleus.

In mammals, as the lens ages, the crystallins form high molecular weight aggregates and become insoluble (Hoender et al. 1981) In the Orange Roughy our SDS-PAGE and Western blot analyses reveal that the insoluble fraction (SDS -soluble fraction) of the nucleus contains beta crystallins which are not present in the equivalent fractions of younger nuclei. This observation provides support for the hypothesis that beta crystallin as well as gamma crystallins are synthesized in fish younger than 18 cm long. The percentage of cortical protein remaining in the nucleus provides a rough estimate of which peaks are disappearing fastest. The data suggests that the high molecular weight peaks #2 and #3 (beta and alpha crystallins) are the least stable, whilst the the low molecular weight peaks #6 + #7 are the most stable. Thus the hypothesis of increasing insolubility with age of high molecular weight crystallin aggregates is supported.

7. Growth and Ultrastructure of the Lens

7.1 Procedures

Size measurements Fresh Orange roughy eye capsules were dissected on board ship. Lenses were removed and washed to remove aqueous humor and dissected free of their suspensory ligaments. The lenses were placed in Tris buffer at pH 6.8 and immediately measured to determine the lens diameter under saline. A Zeiss dissecting microscope with calibrated ocular micrometer was used for this measurement. A restraining device was used to prevent movement of the lens under motion of the ship.

The diameter of fresh wet lenses held at 18° C was measured for each fish before the lenses were frozen for subsequent biochemical assays.

Electron microscopy : Additional fresh Orange roughy eye capsules were dissected on board ship and preserved for electron microscopy, using 3% Glutaraldehyde fixative, buffered at pH 6.8 with 0.175M sodium cacodylate and 0.025MCa^{2+}. Lenses preserved in this fixative were dissected, dehydrated to 100% acetone and critical-point dried, before examination in a Philips 515 scanning electron microscope (CSIRO Hobart). Preserved lenses were dissected using a razor blade, before metal coating for scanning electron microscopy.

7.2 Observations

7.2.1 Lens Size

The measurement of wet lens diameter revealed a change in lens size that was related to other growth parameters, such as standard length. The relationship of lens diameter to the standard length of the fish is shown in **Figure 7.1.** Female fish between 18cm and 42 cm long were selected for these measurements. The data set forms Table 7.1. The relationship between lens diameter and fish length is nearly linear within the sizes measured. Unfortunately smaller fishes were not captured on the cruise.

Table 7.1 Eye Lens Diameters and Otolith Weights for Female Orange Roughies between 18 and 42cm long.

	Length	Otolith wt	Lens diam.	Station code
1	42.000	0.417	17.000	26*5
2	40.000	0.305	17.600	17*1
3	38.000	0.284	17.200	26*1
4	37.000	0.237	16.500	4*1
5	35.000	0.215	15.400	26*12
6	33.000	0.236	15.700	17*10
7	32.000	0.142	14.200	17*8
8	31.000	0.124	13.700	26*9
9	30.000	0.121	14.100	10*1
10	29.000	0.101	13.200	26*3
11	27.000	0.060	12.900	17*9
12	25.000	0.051	11.200	17*2
13	22.000	0.037	10.000	17*5
14	20.000	0.039	9.700	17*7
15	18.000	0.022	7.800	10*2
16	0.000	0.000	0.000	

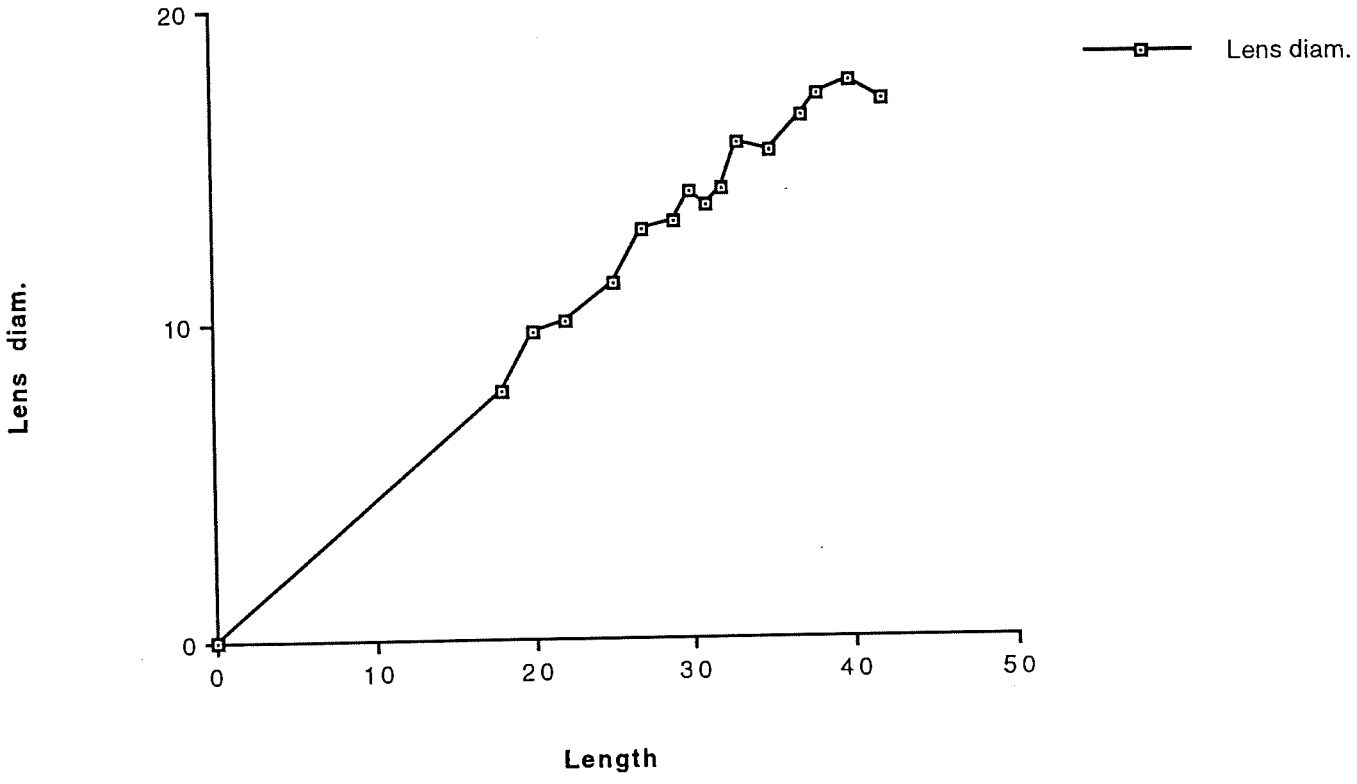

Figure 7.1 Lens Diameter (mm) plotted against Fish Length (cm)

7.2.2. Lens Ultrastructure.

The major structural subdivisions of the lens are shown in **Figures 7.1-7.8. Figure 7.1** is a low power scanning electron micrograph of a bisected lens from a small (18cm long,*St10/2*) fish. The critical point dried lens has a diameter of 5.5mm, indicating a 30% shrinkage from the measured fresh wet diameter of 7.8 mm. This micrograph gives an indication of the difference in packing stucture of proteins in the lens nucleus and cortex, although the fractures in the specimen are drying artifacts. A lens suspensory ligament appears at the lower right of the micrograph.

The lens is made up of tightly packed interdigitating cells. The cells are flattened and extended laterally into finger-like projections which interdigitate with the projections on neighbouring cells. **Figure 7.2** (30cm female *st 10/1*) shows a surface view of the lens cells, indicating the tendency for the lens to separate between the cell layers, and occasionally to fracture across cell layers. **Figure 7.3** shows a lateral view of a lens fracture plane, with cell projections facing the viewer. The tendency of cells to separate as the lens dries out is well seen here. **Figure 7.4** shows the ultrastructure of a group of five or so lens cells, with one folded back to give an impression of cell shape. Note that the lateral projections of each cell in turn bear rows of small papillae, and these papillae also stud the flattened surface of the cells. The interdigitation of adjacent cell projections results in a surprisingly uniform layer of cytoplasm, and presumably contributes to the uniform optical properties of the lens.

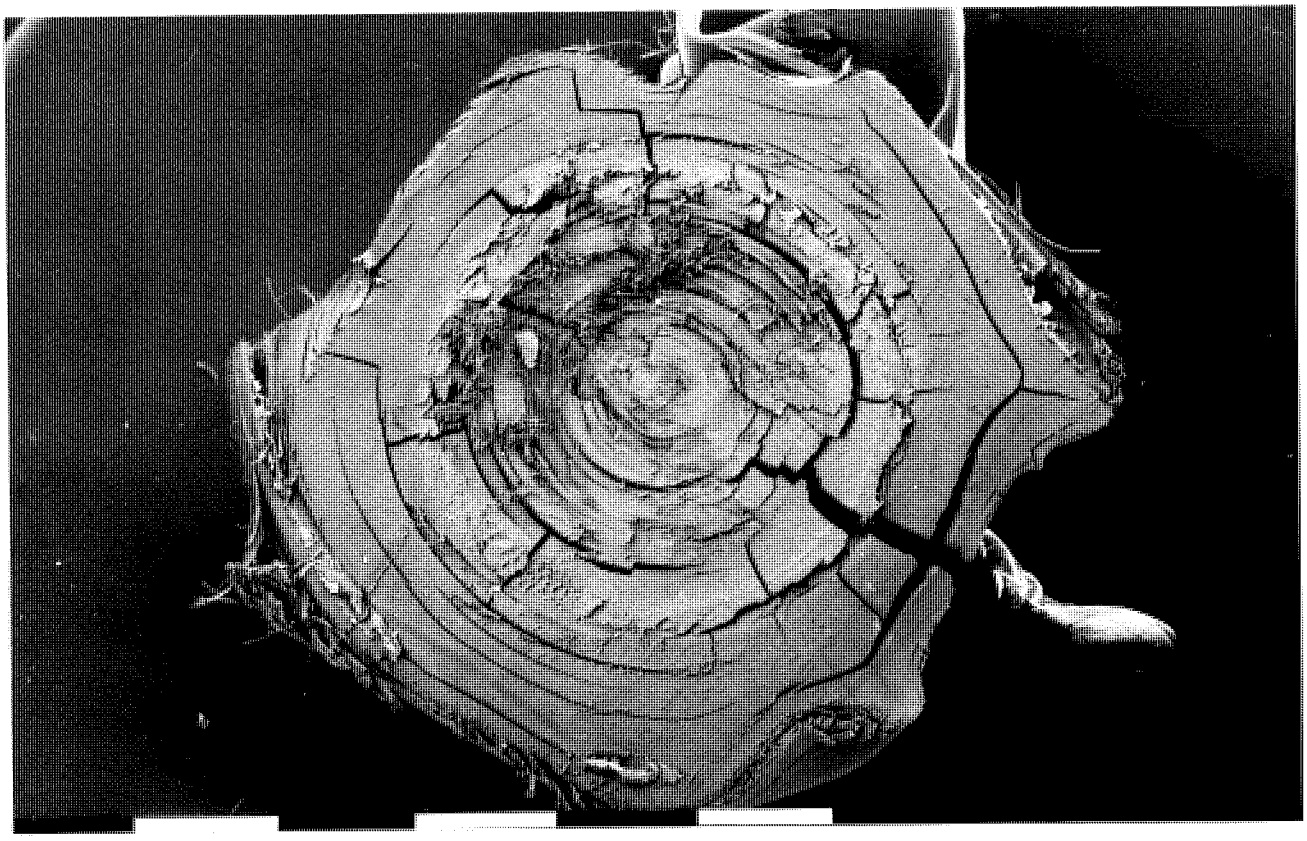

Figure 7.1 SEM of bisected eye lens from 18 cm long female orange roughy. Scale bars 1 mm divisions. See text.

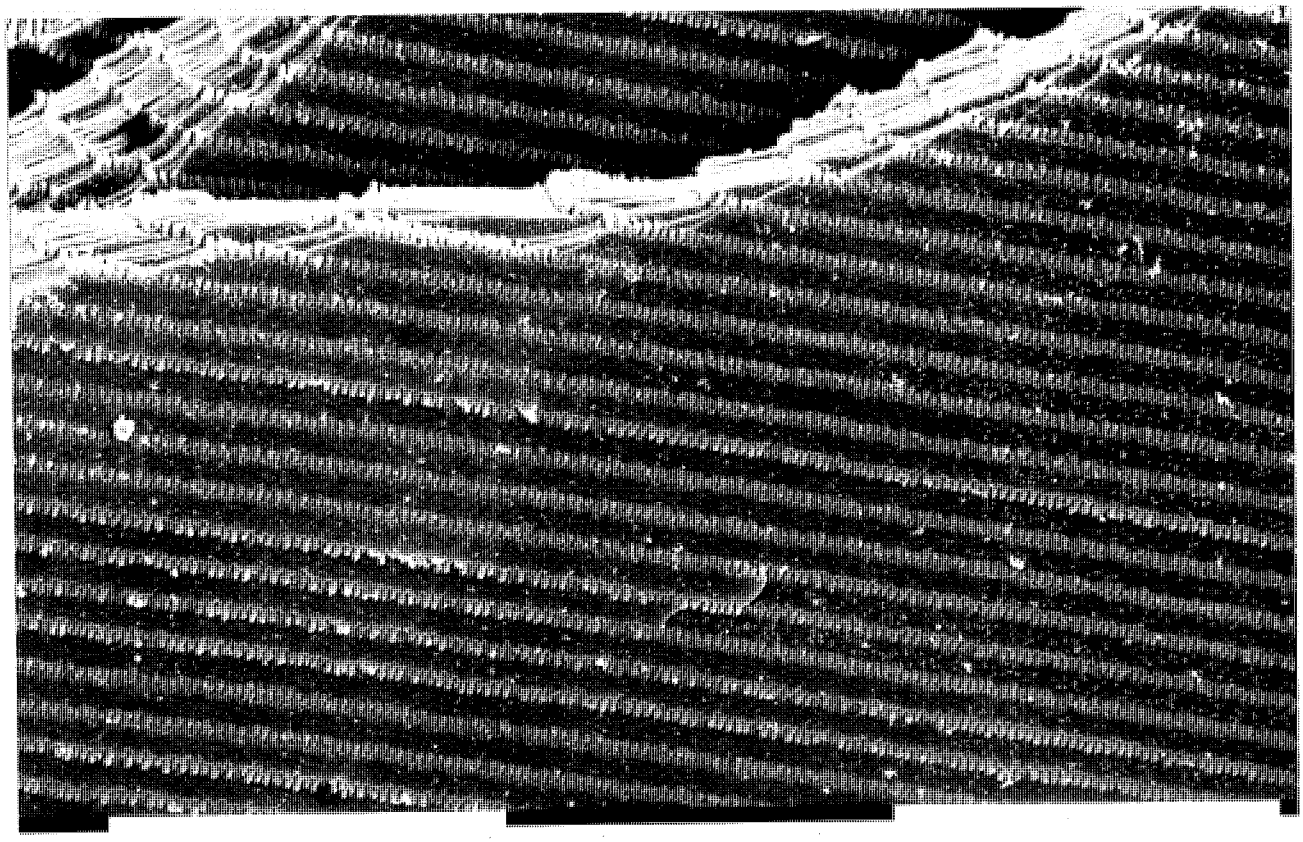

Figure 7.2 SEM of lens cells from a 30 cm female orange roughy. Two fracture planes run across the top of the micrograph, giving an indication of the packing arrangements of the interdigitating lens cells. Scale bars represent 0.1mm.

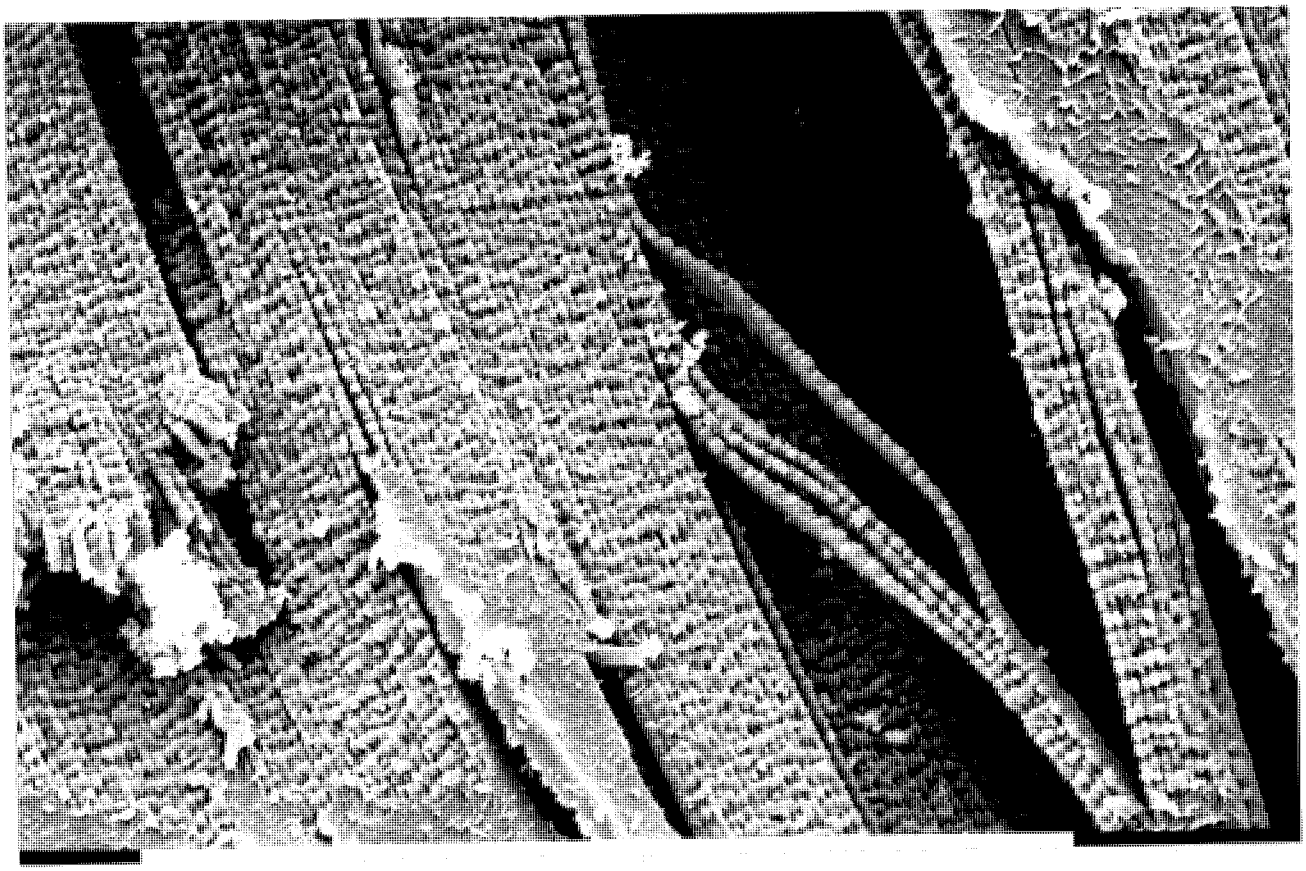

Figure 7.3 SEM showing lens cells in lateral view at a fracture plane. (18 cm female orange roughy). Scale bars represent 0.1mm.

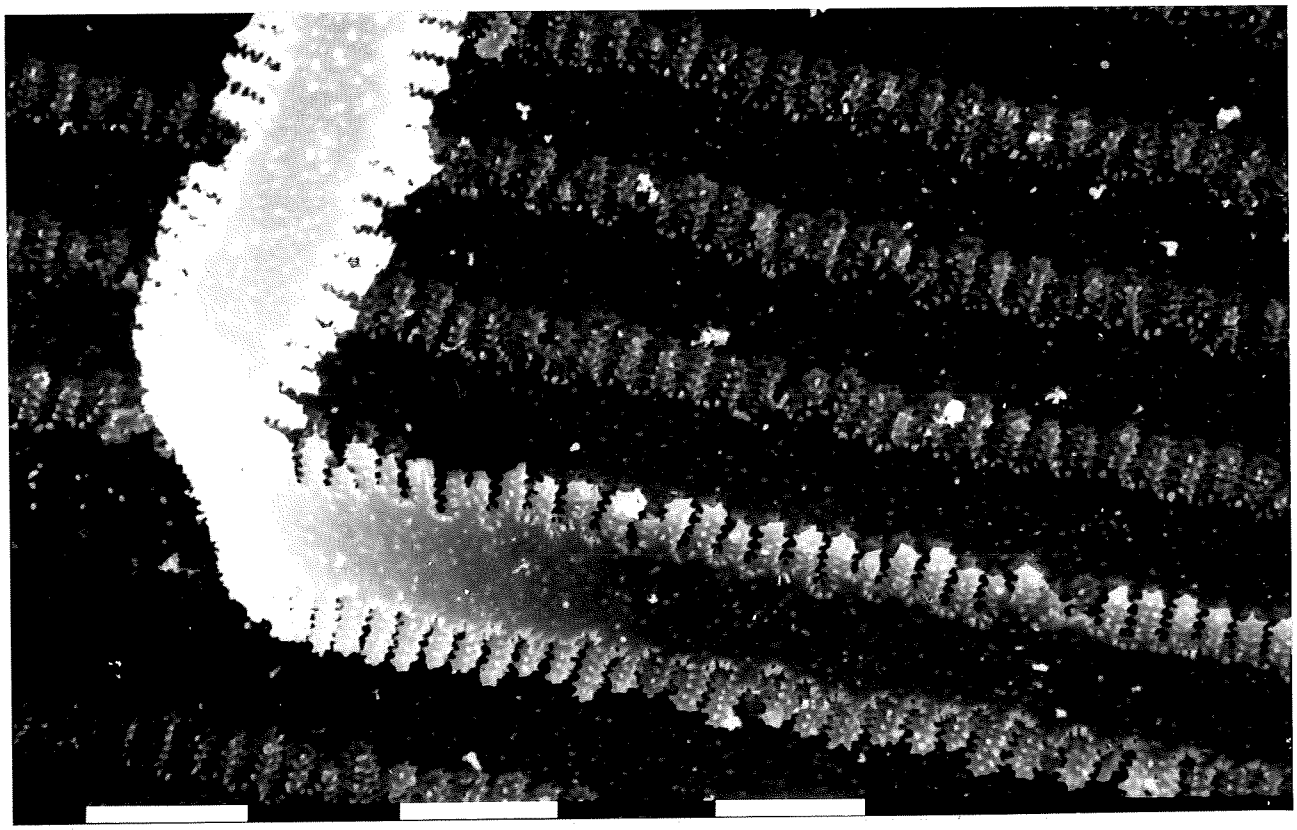

Figure 7.4 SEM showing the interdigitation of lens cells, with close packing of the lateral projections. Note the rows of papillae on the lateral finger-like projections of each lens cell. See text. (30 cm female orange roughy) Scale bars represent 10 micrometre divisions.

8 Changes in the Otolith

8.1 Procedures

Left and right sagittal otoliths were dissected from each individual used in the study of eye lenses, and processed individually. The otoliths were washed repeatedly to remove the organic sheath of the otolith, then air dried at room temperature before weighing. Individual otoliths were weighed to the nearest 0.1mg.

In preparation for electron microscopy, selected otoliths were mounted on glass using epoxy glue and sputter coated with platinum under vacuum. Micrographs were prepared using a secondary emission detector on a Philips 515 scanning electron microscope.

8.2 Electron Microscopy

Scanning electron micrographs of entire orange roughy otoliths are included as **Figures 8.1- 8.7**. **Figure 8.1** shows the right otolith from a female fish 20cm long, weighing 0.30 kg.(17*7). Note profile of the otolith from this small fish, with spade-like anterior edge, and a single lateral projection. The otolith is 7 mm long and weighs 39 milligrams.

Figure 8.2 shows the right otolith from a female fish 25cm long, weighing 0.40kg (Station17*2). The anterior edge has spead out, and two distinct lateral projections are apparent. The otolith is now 9.3 mm long, and weighs 51 milligrams .

Figure 8.3 shows the right otolith from a female fish 31cm long, weighing 0.95kg (Station 26*9). Three lateral projections are now evident, with the separation of a new projection at the anterior end of the otolith. This otolith weighs 124 milligrams.

Figure 8.4 shows the right otolith from a female fish 35cm long, weighing 1.33Kg (Station 26*12). This otolith weighs 215 milligrams, with overall growth and thickening.

Figure 8.5 shows the right otolith from a female fish 42cm long, weighing 1.92kg (Station 26*5). This is a lateral view. Note that a small fragment has been chipped from this otolith during preparation for microscopy. In all examples the opposite (i.e. the left) otolith was intact and was used in preparation of otolith growth data presented in Section 8.3 below. This otolith from a large fish shows the development of complex distal projections, especially posteriorly. The weight of the left otolith from the same fish was 417 milligrams.

Figure 8.1 shows the otolith from a female fish 20cm long, weighing 0.30 kg.(*17*7*). The proximal suspensory facet of the otolith is at the lower edge of the frame. Scale bars represent 1mm.

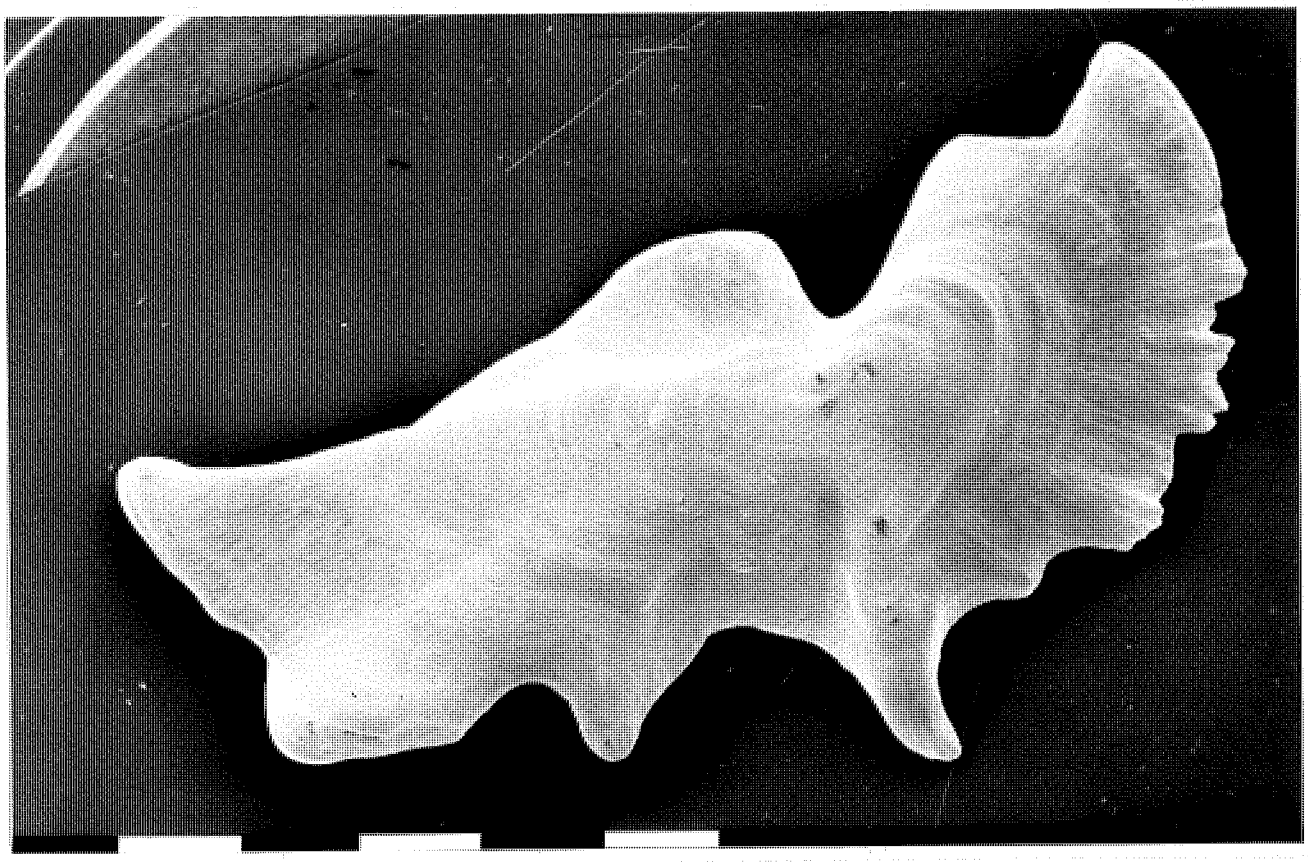

Figure 8.2 Right otolith from a female fish 25cm long, weighing 0.40kg (Station17*2). The proximal suspensory facet of the otolith is at the upper edge of the frame. Scale bars represent 1mm.

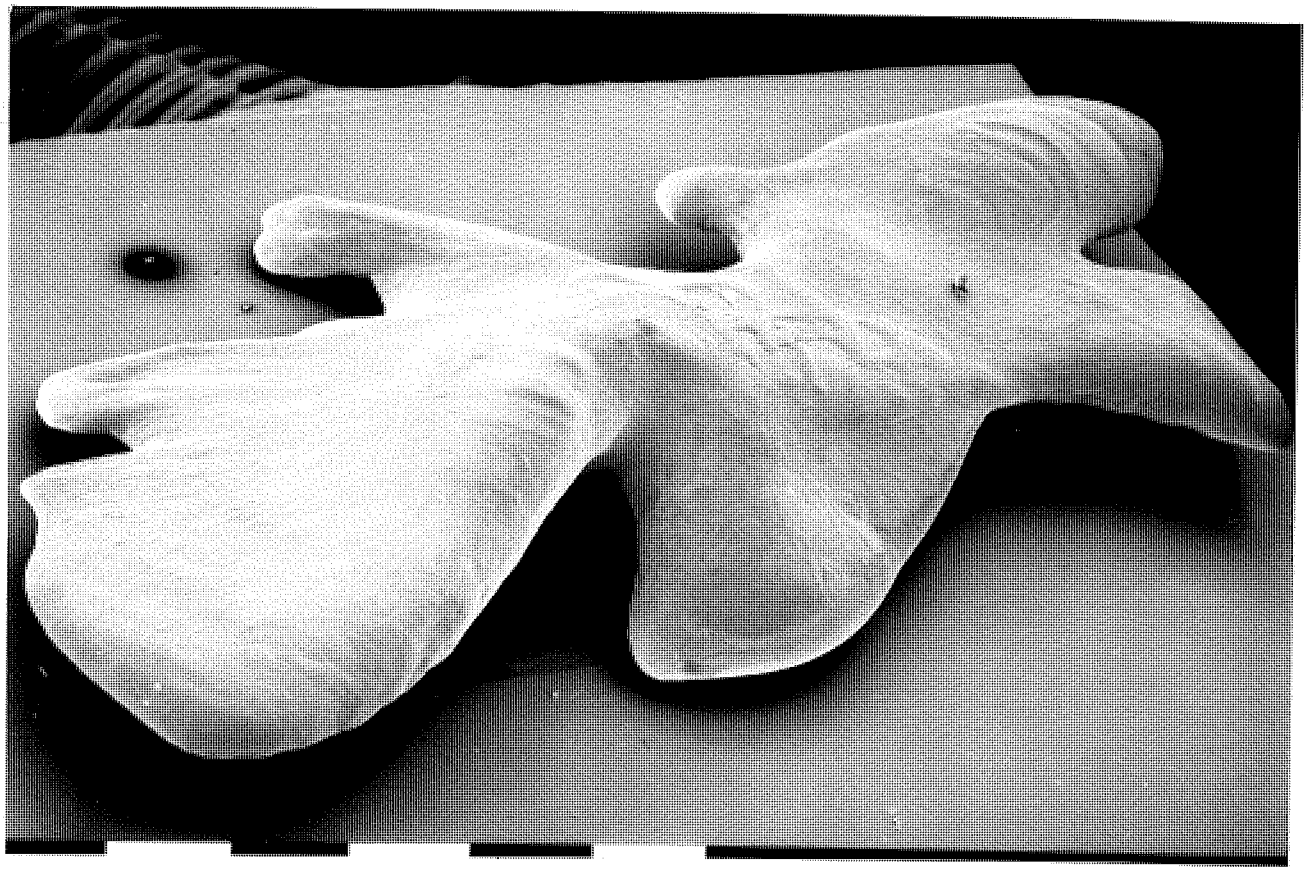

Figure 8.3 Right otolith from a female fish 31cm long, weighing 0.95Kg (Station 26*9). The proximal suspensory facet of the otolith is at the lower edge of the frame. Scale bars represent 1mm.

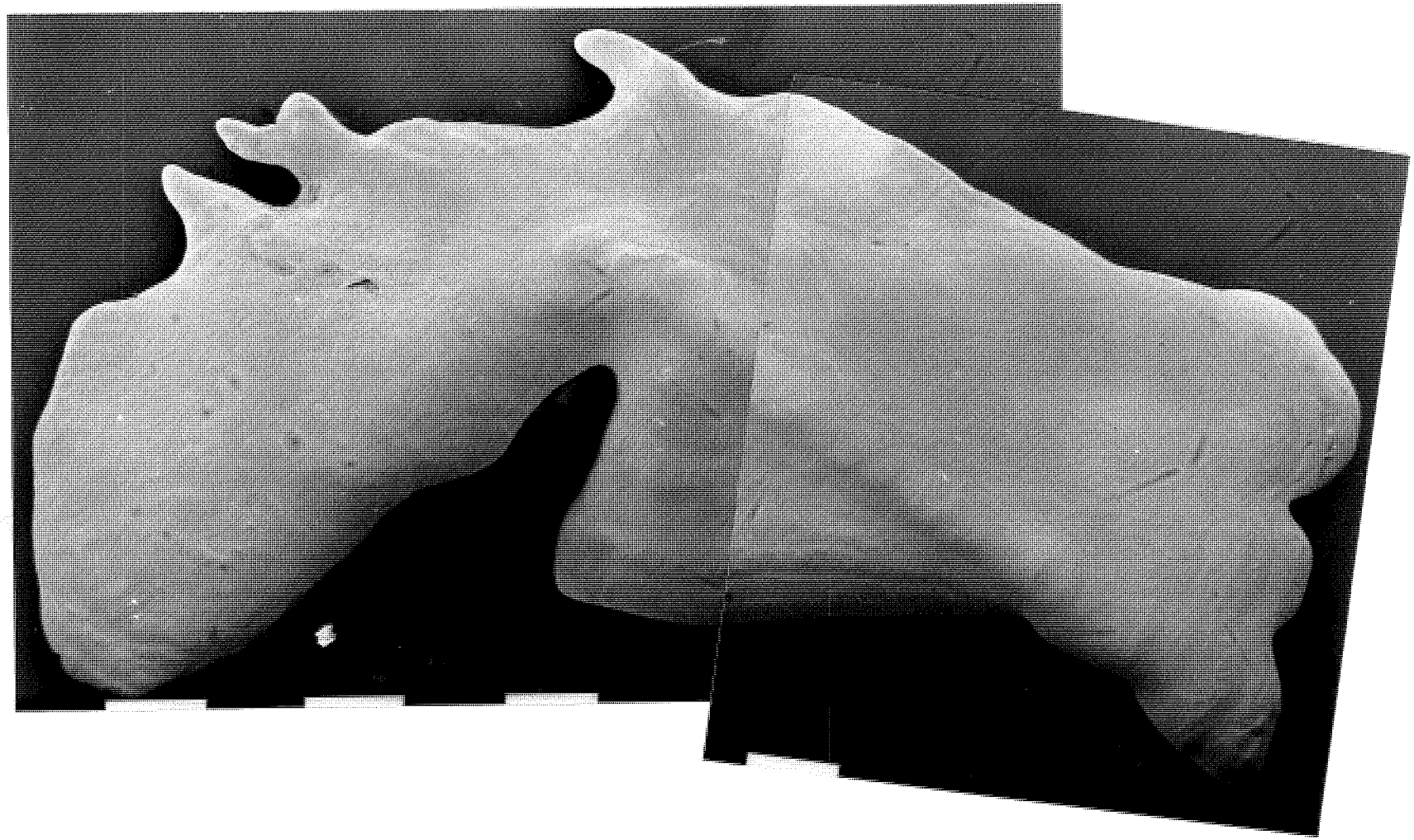

Figure 8.4 Composite of two micrographs showing the right otolith from a female fish 35cm long, weighing 1.33Kg (Station 26*12). Scale bars represent 1mm.

Figure 8.5 Right otolith from a female fish 42cm long, weighing 1.92kg (Station 26*5). This is a lateral view, with the suspensory facet to the left of the frame. Note that a small fragment has been chipped from this otolith during preparation for microscopy.

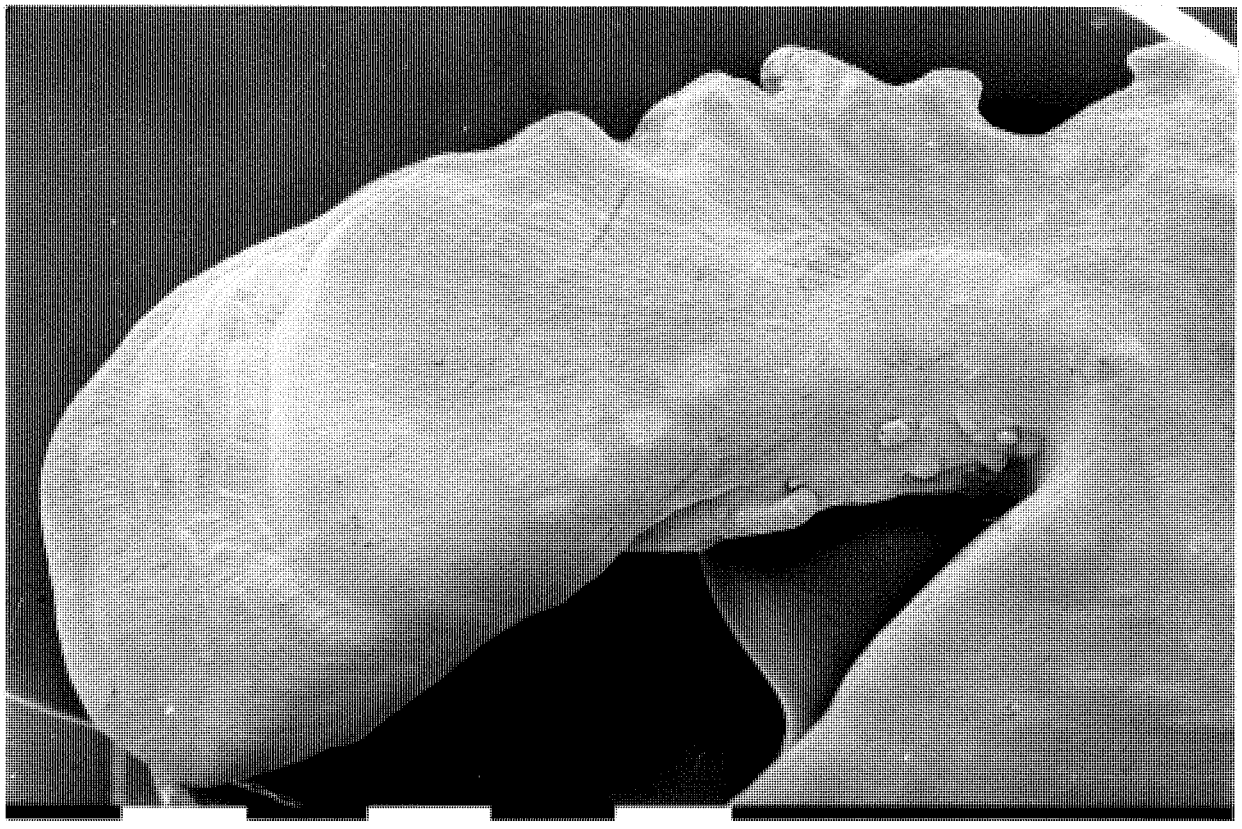

Figure 8.6 Right otolith from a female fish 42cm long, weighing 1.92kg (Station 26*5). Scale bars represent 1mm.

As the otolith grows it becomes larger, heavier, and more complex in profile. The proximal region, adjacent to the suspensory ligament, is least altered with growth, but the distal region develops numerous club- like extensions. These extensions are best developed posteriorly (See **Figure 8.5** for a 42 cm long fish). Small mounds also develop proximally in the cleft adjacent to the nucleus of the otolith, (**Figure 8.6** , for a 42 cm fish (26*5) shows these well).

In the earlier stages of growth, escarpments appear on the growing region of the otolith, and may represent seasonal changes in metabolism. Several figures show these escarpments, e.g. **Figure 8.6**. Daily growth rings cannot be detected on the external surface of orange roughy otoliths, and a series of specimen otoliths have been set aside for future examination using the techniques of X-ray microanalysis. These examinations had not been undertaken at the time of this report.

8.3 Growth Relationships

Relationships between otolith growth, eye lens growth, and fish growth are apparent in **Table 7.1**, where otolith growth is expressed in terms of weight in grams. These relationships are presented graphically in **Figures 8.7- 8.8**.

Figure 8.8 shows a regression curve of the otolith weight as a function of fish standard length. Only female fishes are included in this data. Increase in weight of the otolith is relatively linear until the fish reach about 28cm standard length. Thereafter the otolith weight begins to increase more rapidly than fish standard length, and the weight of individual otoliths becomes more variable. It seems likely that otolith weight may bear a more direct relationship to fish age than does standard length, as discussed below.

8.4 Discussion

The growth of fish otoliths, as determined by measurement of otolith length, generally slows after maturity is reached (Panella 1980), and continues at a reduced rate until maximum fish size is acheived (Williams and Bedford 1974). After maturation the thickness and hence weight of the otolith increases (Boehlert 1985). In the present data for female orange roughy, a discontinuity in growth rate at about 28cm standard length is detected. Similar results were obtained by Fenton et al (1991), although their data for otolith weight plotted against standard length appears to include both male and female fish. Size-frequency analysis of orange roughy populations has indicated that female fish grow larger than male fish (Mace et al 1990).

Maturity for female orange roughy corresponds to a fish standard length of ca.30 cm, but the estimates of the actual age of such fish vary with the methodology (Fenton et al 1991). Unvalidated estimates of age at maturity of 5-12 years have been obtained by counting growth rings on the surface of otoliths (Mace et al 1990), but the radiometric analysis of Fenton et al (1991) indicate an age at maturity of about 32 years (32 cm standard length) for female fish.

A large variation in the weight of sagittal otoliths from adult fish was noted by Fenton et al (1991), ranging between 150 and 430 milligrams. In the present data for female fish, there is also variation, particularly in fish between 28 and 35 cm standard length. It is possible that otolith weight (with regard to gender) may represent a simple methos of estimating fish age, once an age validation can be agreed. Further work on this (important) point will be needed, but cannot be included in the present report.

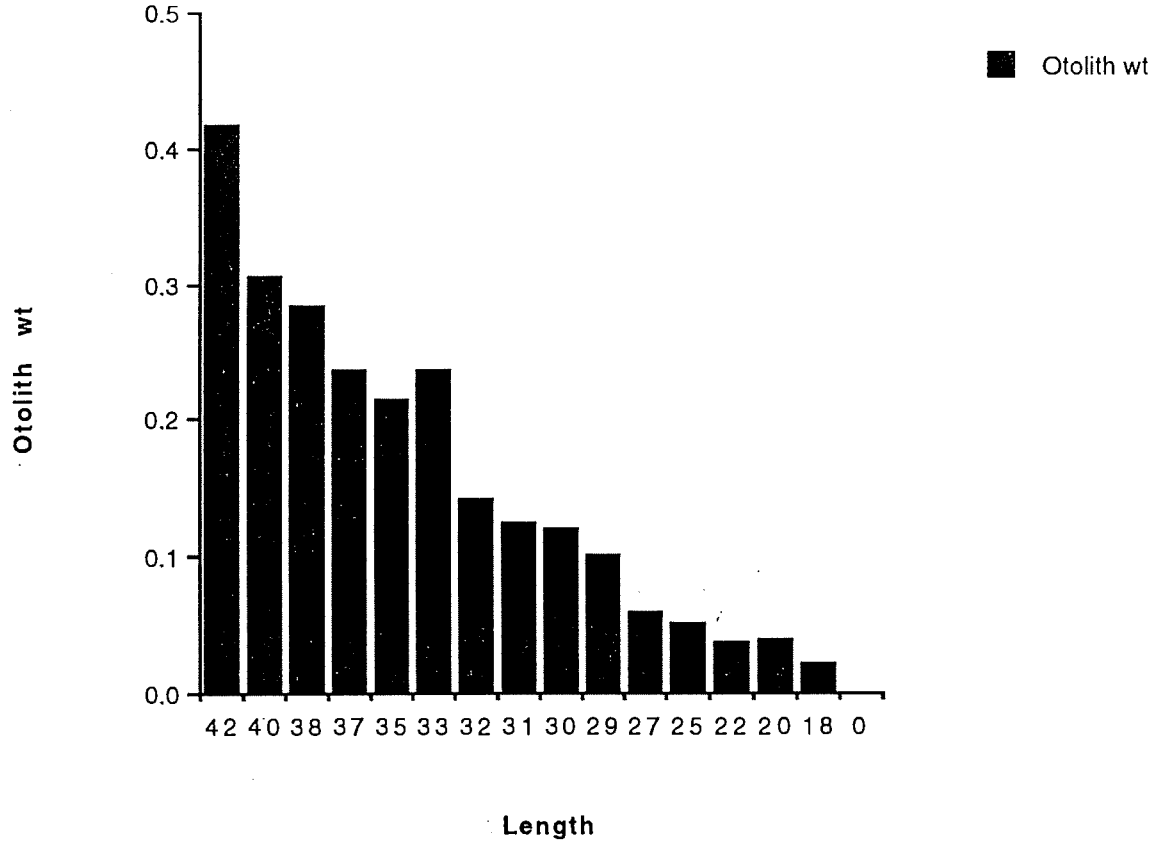

Figure 8.7 Otolith Weight (gm) plotted against Female fish Standard Length (cm).

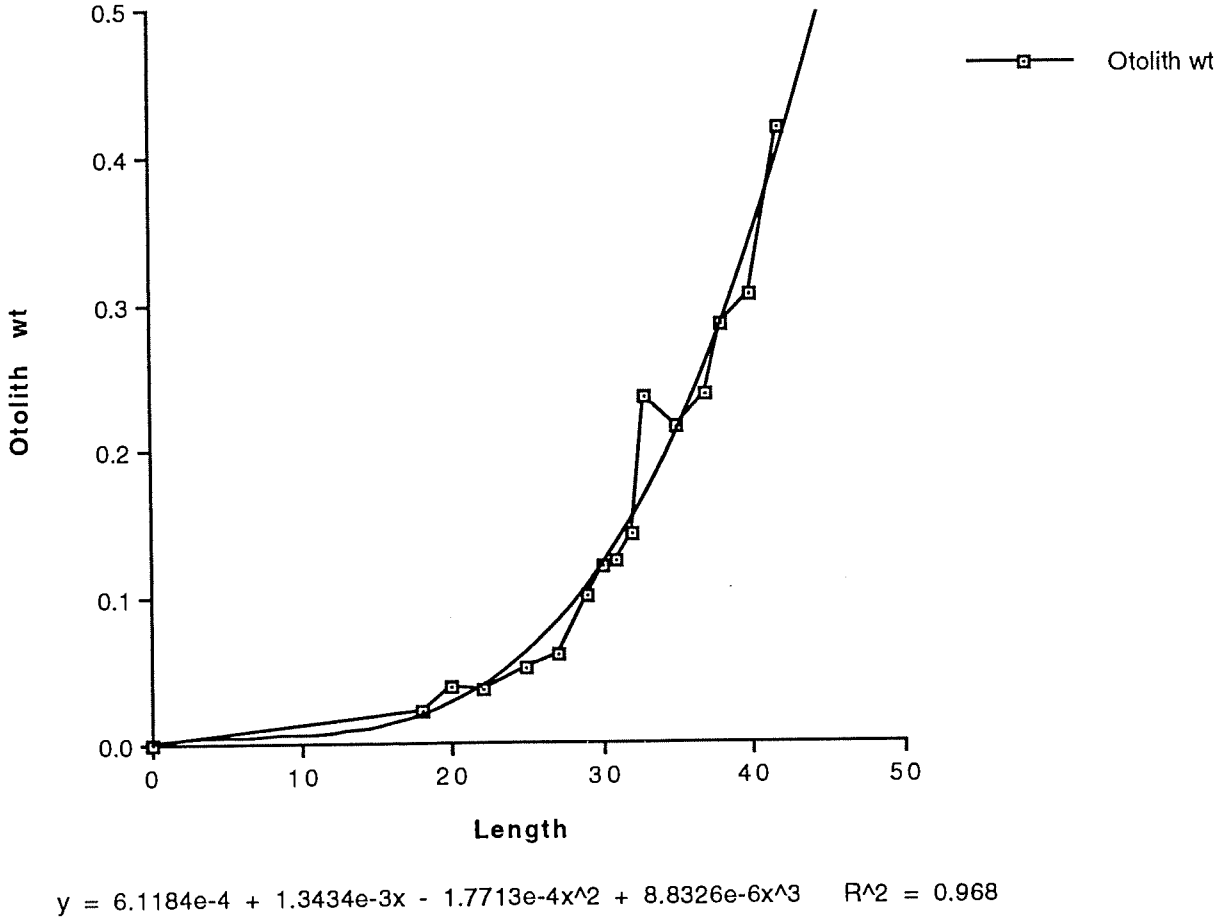

Figure 8.8 shows a regression curve of the otolith weight as a function of fish standard length. Only female fishes are included in this data.

9. References

Boehlert G.W. (1985) Using objective criteria and multiple regression models for age determinatipon in fishes Fish. Bull. U.S. 83, 103-117.

Coombs, S.H. (1981) A density-gradient column for determining the specific gravity of fish eggs, with particular reference to the eggs of the mackerel *Scomber scombrus* Marine Biology, 63, 101-106

Coombs S.H. ,C.A. Fosh and M.A. Keen (198) The bouyancy and vertical distribution of eggs of sprat (*Sprattus sprattus*) and Pilchard (*Sardina pilchardus*) J. mar. biol. Ass. U.K. 65 , 461-474.

Fenton G.E., S.A. Short and D.A. Ritz (1991) Age determination of orange roughy, *Hoplostethus atlanticus* (Pisces: Trachichthyidae) using 210Pb:226Ra disequilibria. Mar. Biol. 109,197-202.

Hart N.H. and M. Donovan (1983) Fine structure of the chorion and site of sperm entry in the egg of *Brachydanio* .

Haug T., E. Kjørsvik and p. Solemdal (1984) Vertical distribution of Atlantic Halibut (*Hippoglossus hippoglossus*) eggs. Can. J. Fish. Aquat. Sci. 41, 798-804.

Mace, P.M. Fenaughty, J.M., Coburn, R.P., Doonan,I.J. (1990) Growth and productivity of orange roughy (*Hoplostethus atlanticus*) on the North Chatham Rise N.Z. Jl. mar. Freshwat. Res. 24, 105-119.

Pannella ,G. (1980) Growth patterns in fish sagittae. In : Rhoads, D.C., Lutz, R.A. (eds) Skeletal growth of aquatic organisms: biological records of environmental change. Plenum N.Y. p.519-560.

Sundby S. (1991) Factors affecting the vertical distribution of eggs. ICES mar. Sci. Symp. 192, 33-38

Williams, R. Bedford, B.C. (1974) The use of otoliths for age determinations. In Bagenal, T. (ed) The ageing of fish. Unwin Bros. Surrey, England., p 114-124.

Acknowledgements

I should like to express my sincere thanks to Dr Roy Harden Jones, and Dr Peter Young who, as Chiefs of the CSIRO Division of Fisheries Research, provided facilities , research ship time, and encouragement throughout the project. I am also particularly grateful for the assistance provided by Dr Tony Koslow and his team in assisting me with my work on orange roughy, and to Dr Tim Davis for his encouragement in my work on tuna larvae.

Section 6 of this report, on ageing in eye lenses of orange roughy was a collaborative project between myself and Sophie Dove of the School of Biological Sciences, University of Sydney. I express here my sincere thanks to Sophie for her painstaking and intelligent work, and for her assistance in the preparation of section 6 of this report.

Appendix 1 -RTTP Cruise- Collection of Pacific Ocean Tuna Larvae

A.C. Crossley joined the RTTP vessel Te Tautai on 26th June 1990 and left the ship on 6th July 1990.

On arrival a 0.65 square metre plankton sampling net was rigged using the portside boom, and tested at 2-3 knots towing speed whilst turning slowly to port. A satisfactory procedure was established , and a total of 21 ring net samples were obtained from surface waters as detailed in Station Data included below. Subsamples were sorted immediately and preserved in glutaraldehyde fixative for electron microscopy, and processed to a stable condition on board Te Tautai. Most samples contained numerous fish larvae and eggs as well as general plankton. All tuna larvae and some other pelagic fish larvae were preserved for later identification in the laboratory. A total of 44 tuna larvae were identified and preserved for electron microscopy .

Many larvae were from unidentified reef fish species, especially in samples taken close to reefs. Some Gempylid and Holocentrid larvae were also preserved for electron microscopy.

Species identification by pigmentation and general anatomy and meristics indicated that of the tuna larvae :

24 (54%) were *Thunnus albacares*

4 (9%) were *Thunnus obesus*

5(11%) were tuna species too small or anomalous for certain identification.

8 (18%) were *Katsuwonus pelamis*

2 (4%) were *Auxis* sp.

1 (2%)was *Sarda* sp.

Although the numbers of larvae caught were small, it may be of some interest to make a comparison with the numbers of adult fish caught by poling and released during the same period, *T. albacares* 806 (30.5%) *Katsuwonus pelamis* 1814 (68.7%)and *T.obesus* 22 (0.8%). It is noted that relatively more *T. albacares* adults were poled in the southern zone, where relatively more *T.albacares* larvae were sampled.

The data obtained on this cruise forms part of a larger study of Scombroid larvae in which collections from the Indian and Pacific Oceans are to be compared. I have a reference collection of scombrid larvae from Yasuo Nishikawa derived from Far Seas Fisheries Research Laboratory cruises.The samples from Palau waters are of particular interest in that they contain larvae which key as *T. albacares* and *T. obesus* using Nishikawa and Rimmer (1987) criteria, but *T.maccoyii* are unlikely to be spawning in this area and this enables me to identify this species with more certainty in my samples from the Java Sea. *T.maccoyii* and *T.obesus* are particularly difficult to distinguish as small larvae, and scanning electron micrographs help. Samples collected on this cruise will be included in a general atlas of larval structure in preparation.

Improved identification of these species is likely to facilitate study of reproduction and recruitment in tunas.

Scanning electron micrographs of larvae sampled during the RTTP programme are attached to this report. Micrographs of certain crustacean species (especially sapphyrids) were prepared for a taxonomic study.

Samples of adult tuna muscle were also taken for high pressure liquid chromatography analysis. These samples will form part of a study of muscle protein changes on ageing, which is still in progress.

Specimens of Atherenidae (baitfish) were collected and delivered to Dr Walter Ivanoff, Macquarie University for taxonomic studies.

RTTP Cruise, Depart Palau, 26 June 1990.
Vessel : Te Tuatai T2FA, Master : Iefata Paeniu
Cruise : Palau 1
Station Catch reports - Ring net and biologicals
Author : Associate Professor A.Clive Crossley.
Date of Report 14/3/92
Author's Sample set #92

STATION DATA

Station A 27/6/90 18.00hrs 6°38' N 133° 55' E Sea Temp 29.2 ° C
Speed 3K. Depth : Surface -3M. Ring net test .
Catch ; Misc Plankton 5 fish larvae (not Scombridae) + 2 scombrid larvae.
Fixation : 92A1 Bulk sample

Station B 28/6/90 09.15hrs 5°55' N 133° 10' E Sea Temp 29.7° C.
Speed 3K. Depth : Surface -3M. Ring net .
Catch ; Misc Plankton , reef fish larvae (not Scombridae) + 5 scombrid larvae.
Fixation : 92B1 *Katsuwonus pelamis* larva <6mm
92B2 *Katsuwonus* larvae (3) <4 mm
92B3 *Katsuwonus* post larva 12mm
92B4 *Thunnus obesus* larva 5 mm
92BG General plankton. Sapphirids, Foraminifera,

Station C 28/6/90 13.45 hrs 5°15' N 132° 50' E Sea Temp 30.2 ° C
Speed 2.5K. Depth : Surface -3M. Ring net .
Catch ; Misc Plankton, fish larva (not Scombridae) .Fish eggs, gastropod veliger larvae, foraminifera, reef fish larva not ID.
Fixation : 92C Bulk plankton sample. Radiolaria, Molluscs.

Station D 28/6/90 19.30 hrs 4°41' N 132° 31' E Sea Temp 29 ° C
Speed 2.5K. Depth : Surface -3M. Ring net .

Catch ; Mixed Plankton, fish larvae (not Scombridae) not ID.Fish eggs.
Fixation : 92D Bulk plankton sample.

Station E 28/6/90 23.00hrs 4°10' N 132° 20' E Sea Temp 29.7° C.
(off Malik Island 6 miles)
Speed 3K. Depth : Surface -3M. Ring net .
Catch ; Misc Plankton , reef fish larvae (not Scombridae)
Fixation : 92E1 Bulk sample.
92E2 *Thunnus albacares* larva

Station F 29/6/90 05.15hrs 3°20' N 131° 55' E Sea Temp 28.9° C.
Speed 3K. Depth : Surface -3M. Ring net .
Catch ; Misc Plankton , reef fish larvae (not Scombridae) + 1 scombrid larva, many Sapphiridae.
Fixation : 92F1 *Katsuwonus* larva <6mm
92F2 Sapphiridae
92FS mollusc shells

Station G 29/6/90 11.30hrs 2°55' N 131° 50' E Sea Temp 28.8° C.
(Off Helen Island) . Speed 3K. Depth : Surface -3M. Ring net .
Catch ; Misc Plankton , reef fish larvae (not Scombridae) + 5 scombrid larvae, decapod larvae.
Fixation : 92G1 *Katsuwonus* larva <6mm
92G2 *T.albacares* larvae (2) <6mm, 1 dissected to expose otolith
92GO *T.albacares* larva, decapod larvae.

Station H 29/6/90 13.30hrs 2°50' N 131° 50' E Sea Temp 29.2° C.
(Off Helen Island) . Speed 2.5K. Depth : Surface -3M. Ring net .
Catch ; Misc Plankton , reef fish larvae (1 Scombrid), fish eggs.
Fixation : 92H1 Reef fish larvae.
92H2 Fish eggs.
92H3 *T.obesus ?* larva

Station I 30/6/90 08.30hrs 2°55' N 131° 50' E Sea Temp 28.8° C.
(Off Helen Island) . Speed 3K. Depth : Surface -3M. Ring net .
Catch ; Misc Plankton , reef fish larvae (not Scombridae) + 5 scombrid larvae, decapod larvae.
Fixation : 92 I 1 *T. albacares* larva <7mm + crustacea
92 I 2 *T. albacares* larva <7mm + sapphirids
92 I 3 Gempylid larva <9 mm
92 I O Reef fish larvae

Station J 30/6/90 12.30hrs (4 miles N of Tobi Island) Sea Temp 28.8° C. Speed 10.5K.
Tuna hooked to deck. Muscle samples taken for High Pressure Liquid Chromatography. Otolith also sampled.

Fish SK1 - skipjack length 393 mm Wt. 1.2 kg. Sex M.
Fish YF 1 - yellowfin length 516 mm Wt 2.6 kg Sex M.

Station K 30/6/90 16.30hrs 3°10' N 132° 05' E Sea Temp 28.4° C.
Speed 3K. Depth : Surface -3M. Ring net .
Catch ; Misc Plankton , reef fish larvae , soldierfish larvae (not Scombridae)
Fixation : 92 K

Station L 1/7/90 05.30hrs 4°20' N 132° 15' E (off Merir Island)
Speed 3K. Depth : Surface -3M. Ring net .
Catch ; Misc Plankton , decapod larvae, reef fish larvae
Fixation : 92 L

Station M 1/7/90 . 11.15hrs 5°05' N 132° 30' E .
(Off Sonsorol Island) . Speed 3K. Depth : Surface -3M. Ring net .
Catch ; Misc Plankton , reef fish larvae (not Scombridae), 2 *Holecentrus spp* larvae + 1x 7mm *K. pelamis* larva , fish embryos.
Fixation : 92 M 1 *K. pelamis*
92 M 2 *Holocentrus* larvae
92 M 3 fish embryos

Station N 2/7/90 . 09.15hrs 6°57' N 134° 06' E Sea Temp 29.0° C.
(Off Angaur Island) . Speed 2K. Depth : Surface -3M. Ring net .
Catch ; Misc Plankton , reef fish larvae (not Scombridae), *Holocentrus spp* larvae + 13 scombrid larvae, 9 probably *T. albacares.*
Fixation : 92 N 1 *T. albacares* 8 mm
92 N 2 3*Holocentrus* larvae ca 6 mm.
92 N 3 2*T . albacares* 7 mm larvae various pigment patterns.
92 N 4 *Auxis* sp larva
92 N 5 2 *T. albacares* larvae anomalous pigment patterns
92 N 6 *T. albacares* larva anomalous pigment pattern.

Station O 2/7/90 . 12.40hrs 7°05' N 134° 27' E Sea Temp 29.1° C.
(Off Eil Malk) . Speed 2.8 K. Depth : Surface -3M. Ring net , 10 mins.
Catch ; Misc Plankton, esp crustacea radiolaria, 24 reef fish larvae (not Scombridae) +2 *T. albacares* larvae,
Fixation : 92 O 1 *T. albacares* larva
92 O 2 *T. albacares* larva
92 O 3 reef fish larvae

Station P 3/7/90 . 03.00hrs 7°19' N 134° 25' E
(Malakal Harbour ,Palau) . Speed 0K. Baitfish haul . Atherenidae collected for Dr Walter Ivanoff, Macquarie University.

Station Q 3/7/90 . 08.45hrs 7°19' N 134° 27' E
(Inside reef , Palau) . Speed 2K. Depth : Surface -3M. Ring net .

Station R 3/7/90 . 13.00hrs 7°50' N 134° 25' E
(Off Cormoran Reef, Babelthuap Island) . Speed 3K. Depth : Surface -3M. Ring net .
Catch ; Misc Plankton , 14 reef fish larvae (not Scombridae).

Station S 3/7/90 . 17.15hrs 8°02' N 134° 36' E.
(N entrance to Kossai Passage) . Speed 2.5K. Depth : Surface -3M. Ring net
Catch ; Misc Plankton , 50 reef fish larvae (not Scombridae) + x3 scombrid larvae,
Fixation : 92 S 1 *T. albacares* larva
92 S 2 Misc. zooplankton
92 S 3 *Sarda orientalis* larva
92 S 4 possibly *T. alalunga* or anomalous *albacares* larva.

Station T 4/7/90 . 07.25hrs 8°09' N 134° 42' E.
(Off Babelthuap Island) . Speed 2.5K. Depth : Surface -3M. Ring net
Catch ; Misc Plankton , 50 reef fish larvae (not Scombridae) + x3 scombrid larvae,
Fixation : 92 T 1 *Gempilid* larva
92 T 2 *T. obesus ?* larva
92 T 3 *T. albacares* larva
92 T 4 possibly 4mm *T. alalunga* or anomalous *albacares* larvae.
92 T 5 Scombroid larva not identified
92 T 6 Scombroid larva not identified
92 T 7 *Auxis* sp larva
92 T 8 Scombroid larvae not identified

Station U 4/7/90 . 13.50hrs 7°21' N 134° 47' E.
(Off Palau) . Speed 2.5K. Depth : Surface -3M. Ring net
Catch ; Misc Plankton , 10 reef fish larvae (not Scombridae) 4mm *Holocentrus* + x1 scombrid larva.
Fixation : 92 U 1 *T. albacares* larvae

Station V 5/7/90 . 06.30hrs 7°15' N 134° 29' E.
(Outside E entrance to Koror harbour) . Speed 2.5K. Depth : Surface -3M. Ring net
Catch ; Misc Plankton many zoea , 50 reef fish larvae (not Scombridae) ,5 *Holocentrus* larvae
Fixation : 92 V 1 *Holocentrus* larvae

Station W 5/7/90 . 13.35hrs 7°06' N 134° 35' E.
(E entrance to Koror harbour) . Speed 2.5K. Depth : Surface -3M. Ring net
Catch ; Misc Plankton many zoea , 50 reef fish larvae (2 Scombridae) ,5 *Holocentrus* larvae

Fixation : 92 W 1 *T. albacares* larva
92 W 2 *T. obesus* larva

Station X 5/7/90 15.30 hrs (East of Palau Island) Tuna tagging station.

Muscle and eye protein biological samples for HPLC, all *T. albacares*.